Noname manuscript No.
(will be inserted by the editor)

A Non-Intrusive Solution to the Ill-Conditioning Problem of the Gradient-Enhanced Gaussian Covariance Matrix for Gaussian Processes

André L. Marchildon · David W. Zingg

Received: date / Accepted: date

Abstract Gaussian processes (GPs) are used for numerous different applications, including uncertainty quantification and optimization. Ill-conditioning of the covariance matrix for GPs is common with the use of various kernels, including the Gaussian, rational quadratic, and Matérn kernels. A common approach to overcome this problem is to add a nugget along the diagonal of the covariance matrix. For GPs that are not constructed with gradients, it is straightforward to derive a nugget value that guarantees the condition number of the covariance matrix to be below a user-set threshold. However, for gradient-enhanced GPs, there are no existing practical bounds to select a nugget that guarantee that the condition number of the gradient-enhanced covariance matrix is below a user-set threshold. In this paper a novel approach is taken to bound the condition number of the covariance matrix for GPs that use the Gaussian kernel. This is achieved by using non-isotropic rescaling for the data and a modest nugget value. This non-intrusive method works for GPs applied to problems of any dimension and it allows all data points to be kept. The method is applied to a Bayesian optimizer using a gradient-enhanced GP to achieve deep convergence. Without this method, the high condition number constrains the hyperparameters for the GP and this is shown to impede the convergence of the optimizer. It is also demonstrated that applying this method to the rational quadratic and Matérn kernels alleviates the ill-conditioning of their gradient-enhanced covariance matrices. Implementation of the method is straightforward and clearly described in the paper.

Keywords Gaussian process · Covariance matrix · Condition number · Bayesian optimization

André L. Marchildon
University of Toronto Institute for Aerospace Studies, Toronto, ON, Canada
E-mail: andre.marchildon@mail.utoronto.ca

David W. Zingg
University of Toronto Institute for Aerospace Studies, Toronto, ON, Canada

Mathematics Subject Classification (2020) 60G15 · 65K10

1 Introduction

Gaussian processes (GPs) provide a method of constructing probabilistic surrogates [16,18]. The versatility and practicality of GPs have made them popular for various applications. For example, GPs are used for classification [16], for uncertainty quantification [5], and for optimization [20,15]. A GP requires a covariance function and there are a wide variety of kernels that can be used [16,1]. The Gaussian kernel, also known as the squared exponential kernel, is the most commonly used. Some of the attractive properties of this kernel include simplicity, hyperparameters that can be tuned, and its smoothness, which allows for gradients to be used [24].

GPs can be constructed from not only function values but also gradients of the function [15,24,3,25]. Using the gradients to construct the covariance matrix allows for surrogates that not only match the function evaluations, but also its gradient at the evaluation points, thus providing a surrogate that is more accurate [15,25]. The use of gradients is particularly helpful for high-dimensional problems, which are often encountered in optimization [29,6]. The gradients are incorporated into the GP by modifying the structure of the covariance matrix, which is known as the direct method [8,3,24,12]. There is also a less commonly used indirect method that does not require the structure of the covariance matrix to be modified, which also suffers from ill-conditioning [27]. In fields such as geostatistics, Kriging models and gradient-enhanced Kriging models are used [3]. The covariance matrix for a Kriging model typically also uses a kernel and is equivalent to the covariance matrix for a GP.

The problem of ill-conditioned gradient-free covariance matrices for GPs is common for a wide range of kernels [11,28], including the Gaussian kernel [1]. The factors that cause the ill-conditioning of the gradient-free covariance matrix for GPs has been studied in detail in [4]. It was identified that the ill-conditioning problem gets worse as the data points get closer together and the importance of using a nugget to increase the diagonal entries of the covariance matrix was highlighted. The role of the nugget to help alleviate the ill-conditioning of positive definite matrices and GPs specifically is well studied and it is extensively used [17,2,7]. For gradient-free GPs, the use of a nugget is sufficient to ensure that the condition number of the covariance matrix is below a user-set threshold. However, it is impractical to use this approach on its own for gradient-enhanced GPs since it can require a significantly larger nugget, which can negatively impact the accuracy of the surrogate [3]. Furthermore, the gradient-enhanced covariance matrices can be significantly more ill-conditioned than their gradient-free counterparts [9].

Various strategies have been used to mitigate the ill-conditioning problem of gradient-enhanced covariance matrices. For example, a minimum distance between evaluation points was imposed in [15]. This helped alleviate some of the ill-conditioning problems since data points that are close together result

in two rows of the covariance matrix being nearly identical, which causes the matrix to be ill-conditioned. Unfortunately, as the authors highlighted, this constraint is undesirable since data points naturally get closer together as an optimizer gets closer to a minimum. The authors in [24] applied a discrete Fourier transform to modify the application of the covariance matrix. Unfortunately, this method introduced errors due to the lack of periodic boundary conditions, and the storage requirement for the Fourier frequencies was highlighted as a bottleneck. Another method that has been used involves removing function and gradient evaluations from the construction of the covariance matrix until its condition number is below a user-set threshold [13,3]. All of these methods are empirical in nature and do not provide an upper bound on the condition number. Furthermore, these methods generally require that some data points be excluded from the construction of the covariance matrix. The objective of the present paper is to present a method that does not suffer from these drawbacks, is non-intrusive, and is straightforward to implement in existing codes that utilize Gaussian processes.

In Section 2 the notation used in this paper is introduced. The GP and the Gaussian kernel are then presented in Section 3. The role of the nugget to decrease the condition number of the covariance matrix is detailed in Section 4. The ill-conditioning problem for the Gaussian kernel along with the rational quadratic and Matérn $\frac{5}{2}$ kernels is highlighted in Section 5. In Section 6 the condition number of the gradient-free covariance matrix is investigated using Gershgorin's circle theorem. This analysis is repeated in Section 7 for the gradient-enhanced GP. The results from Section 7 are then used in Sections 8 and 9 to derive required values for the nugget and the minimum Euclidean distance between data points to ensure that the condition number of the gradient-enhanced covariance matrix is below a user-set threshold. The required steps to implement the method of ensuring that the condition number of the covariance matrix is below a certain threshold are provided in Section 10. In this same section, an optimization test case is presented to demonstrate how the new method allows for deeper convergence to be achieved as a result of the improved conditioning of the covariance matrix.

2 Notation

Consider the function $f(x, y, g(x); d, n_x)$, where x and y are arbitrary variables, $g(x)$ is a nested function, while $d \in \mathbb{Z}^+$ and $n_x \in \mathbb{Z}^+$ are parameters that indicate the dimension and the number of evaluations in the parameter space, respectively. When a function $f(x, y, g(x); d, n_x)$ is presented as $f(x, g(x))$, the omitted variables and parameters are implicitly held constant. A variable with an asterisk indicates the value of the variable that maximizes the function. For example, x^* is the value of x that maximizes $f(x, g(x))$. A function with an asterisk indicates that it is maximized with respect to all of its variables, i.e. $f^* = f(x^*, y^*, g(x^*))$. Upper and lower bounds on a function $f(\cdot)$ are indicated as $u_f(\cdot)$ and $\ell_f(\cdot)$, respectively. The lower and upper bounds may

take different arguments than the function they are bounding and are usually not tight bounds, unlike for example f^*, which represents a tight upper bound on f.

Matrices are represented as sans-serif capital letters. For example, I represents the identity matrix. Vectors are denoted in bold font, e.g. $\boldsymbol{x}$ is a vector of length d representing one location in a parameter space. The i-th parameter of the j-th location in the parameter space is represented by $x_j^{(i)}$.

For figures, solid lines are used for functions, dashed lines are for lower and upper bounds, and dotted lines indicate locations of critical points such as the maximum of a function.

3 Gaussian process and Gaussian kernel

When performing tasks such as optimization or uncertainty quantification, a function of interest will be evaluated at a finite number of points in a parameter space. Since the original function can be expensive to evaluate, we are interested in having an inexpensive estimate of this function that can be sampled at any point in the parameter space. A GP provides a surrogate that is normally distributed at each point in the parameter space and is inexpensive to evaluate. A GP requires a mean and a covariance function. The mean function is simply selected to be a constant and we use the popular Gaussian kernel for the covariance function

$$k(\boldsymbol{x}, \boldsymbol{y}) = e^{-\sum_{i=1}^{d} \theta_i \left(x^{(i)} - y^{(i)}\right)^2}, \tag{1}$$

where $\boldsymbol{\theta}$ is a vector of hyperparameters, while $\boldsymbol{x}$ and $\boldsymbol{y}$ are points in the parameter space. To have gradient-enhanced GPs, which are desired for their improved fidelity relative to their gradient-free counterpart [24], we also require the derivatives of the kernel with respect to its inputs

$$\frac{\partial k(\boldsymbol{x}, \boldsymbol{y})}{\partial x^{(i)}} = -2\theta_i \left(x^{(i)} - y^{(i)}\right) k(\boldsymbol{x}, \boldsymbol{y}) \tag{2}$$

$$\frac{\partial k(\boldsymbol{x}, \boldsymbol{y})}{\partial y^{(j)}} = 2\theta_j \left(x^{(j)} - y^{(j)}\right) k(\boldsymbol{x}, \boldsymbol{y}) \tag{3}$$

$$\frac{\partial^2 k(\boldsymbol{x}, \boldsymbol{y})}{\partial x^{(i)} \partial y^{(j)}} = \left(2\delta_{ij}\theta_i - 4\theta_i\theta_j \left(x^{(i)} - y^{(i)}\right)\left(x^{(j)} - y^{(j)}\right)\right) k(\boldsymbol{x}, \boldsymbol{y}), \tag{4}$$

where δ_{ij} is the Kronecker delta. The kernel handles inputs that are matrices as follows

$$k(\mathsf{X}, \mathsf{Y}) = \begin{bmatrix} k(\mathsf{X}_{1,:}, \mathsf{Y}_{1,:}) & k(\mathsf{X}_{1,:}, \mathsf{Y}_{2,:}) & \dots & k(\mathsf{X}_{1,:}, \mathsf{Y}_{n_y,:}) \\ k(\mathsf{X}_{2,:}, \mathsf{Y}_{1,:}) & k(\mathsf{X}_{2,:}, \mathsf{Y}_{2,:}) & \dots & k(\mathsf{X}_{2,:}, \mathsf{Y}_{n_y,:}) \\ \vdots & \vdots & \ddots & \vdots \\ k(\mathsf{X}_{n_x,:}, \mathsf{Y}_{1,:}) & k(\mathsf{X}_{n_x,:}, \mathsf{Y}_{2,:}) & \dots & k(\mathsf{X}_{n_x,:}, \mathsf{Y}_{n_y,:}), \end{bmatrix}, \tag{5}$$

where $\mathsf{X}_{i,:}$, is the i-th row of X, while n_x and n_y are the number of rows in X and Y, respectively.

The matrix X is used to hold the locations where a function of interest and its gradient have been evaluated. The vector $\boldsymbol{x}$ is the location at which the surrogate is evaluated, and the vector $\boldsymbol{f}$ holds the function evaluations at all rows in X. The gradient evaluations at the rows in X form a matrix F_∇ of size $n_x \times d$ that is reshaped into the vector $\boldsymbol{f}_\nabla$ of length $n_x \cdot d$. The mean and variance of the surrogate for the gradient-free case can be evaluated with

$$\mu_f(\boldsymbol{x}) = \hat{\mu}_f + \boldsymbol{k}^T(\boldsymbol{x}) \left(\mathsf{K} + \eta_\mathsf{K} \mathsf{I}\right)^{-1} (\boldsymbol{f} - \hat{\mu}_f) \tag{6}$$

$$\sigma_f^2(\boldsymbol{x}) = \hat{\sigma}_f^2 \left(1 - \boldsymbol{k}^T(\boldsymbol{x}) \left(\mathsf{K} + \eta_\mathsf{K} \mathsf{I}\right)^{-1} \boldsymbol{k}(\boldsymbol{x})\right), \tag{7}$$

where $\boldsymbol{k} = k(\mathsf{X}, \boldsymbol{x})$ and $\mathsf{K} = k(\mathsf{X}, \mathsf{X})$ is the gradient-free covariance matrix. The hyperparameters $\hat{\sigma}_f$ and $\hat{\mu}_f$ are set by optimizing the log-likelihood function, which is presented at the end of this section. Finally, the nugget $\eta_\mathsf{K} \in \mathbb{R}^+$ is used when the data are noisy and it also helps to reduce the condition number of the covariance matrix, as detailed in Section 4.

To evaluate the surrogate with the gradient-enhanced covariance matrix we require

$$\mathsf{K}_\nabla = \begin{bmatrix} k(\mathsf{X},\mathsf{X}) & \frac{\partial k(\mathsf{X},\mathsf{X})}{\partial y^{(1)}} & \cdots & \frac{\partial k(\mathsf{X},\mathsf{X})}{\partial y^{(d)}} \\ \frac{\partial k(\mathsf{X},\mathsf{X})}{\partial x^{(1)}} & \frac{\partial^2 k(\mathsf{X},\mathsf{X})}{\partial x^{(1)} \partial y^{(1)}} & \cdots & \frac{\partial^2 k(\mathsf{X},\mathsf{X})}{\partial x^{(1)} \partial y^{(d)}} \\ \vdots & \vdots & \ddots & \vdots \\ \frac{\partial k(\mathsf{X},\mathsf{X})}{\partial x^{(d)}} & \frac{\partial^2 k(\mathsf{X},\mathsf{X})}{\partial x^{(d)} \partial y^{(1)}} & \cdots & \frac{\partial^2 k(\mathsf{X},\mathsf{X})}{\partial x^{(d)} \partial y^{(d)}} \end{bmatrix}, \quad \boldsymbol{k}_\nabla = \begin{bmatrix} k(\mathsf{X}, \boldsymbol{x}) \\ \frac{\partial k(\mathsf{X},\boldsymbol{x})}{\partial x^{(1)}} \\ \vdots \\ \frac{\partial k(\mathsf{X},\boldsymbol{x})}{\partial x^{(d)}} \end{bmatrix}, \tag{8}$$

where $\boldsymbol{k}_\nabla$ is of length $n_x(d+1)$ and K_∇ is the gradient-enhanced covariance matrix of size $n_x(d+1) \times n_x(d+1)$. The mean and variance of the surrogate model with the gradient-enhanced covariance matrix are calculated with

$$\mu_f(\boldsymbol{x}) = \hat{\mu}_f + \boldsymbol{k}_\nabla^T(\boldsymbol{x}) \left(\mathsf{K}_\nabla + \eta_{\mathsf{K}_\nabla} \mathsf{I}\right)^{-1} \left[\boldsymbol{f}^T - \hat{\mu}_f, \boldsymbol{f}_\nabla^T\right]^T \tag{9}$$

$$\sigma_f^2(\boldsymbol{x}) = \hat{\sigma}_f^2 \left(k(\boldsymbol{x}, \boldsymbol{x}) - \boldsymbol{k}_\nabla^T(\boldsymbol{x}) \left(\mathsf{K}_\nabla + \eta_{\mathsf{K}_\nabla} \mathsf{I}\right)^{-1} \boldsymbol{k}_\nabla(\boldsymbol{x})\right), \tag{10}$$

where $\eta_{\mathsf{K}_\nabla} \in \mathbb{R}^+$. The hyperparameters are commonly selected by maximizing the marginal likelihood [22], which is given by

$$L(\boldsymbol{\theta}, \hat{\mu}_f, \hat{\sigma}_f^2; \mathsf{X}, \boldsymbol{f}, \eta_{\mathsf{K}_\nabla}) = \frac{e^{-\frac{\left[\boldsymbol{f}^T - \hat{\mu}_f, \boldsymbol{f}_\nabla^T\right] \left(\mathsf{K}_\nabla(\boldsymbol{\theta}) + \eta_{\mathsf{K}_\nabla} \mathsf{I}\right)^{-1} \left[\boldsymbol{f}^T - \hat{\mu}_f, \boldsymbol{f}_\nabla^T\right]^T}{2\hat{\sigma}_f^2}}}{\left(2\pi\hat{\sigma}_f^2\right)^{\frac{n_x(d+1)}{2}} \sqrt{\det\left(\mathsf{K}_\nabla(\boldsymbol{\theta}) + \eta_{\mathsf{K}_\nabla} \mathsf{I}\right)}}, \tag{11}$$

where the gradient-free case is analogous and η_{K_∇} is set by the user. It is common to consider the marginal log-likelihood by taking the natural logarithm of L [22]. The optimal values of $\hat{\mu}_f$ and $\hat{\sigma}_f$ can be found by differentiating $\ln(L)$ with respect to these hyperparameters and setting the derivative to zero. As will be shown in Section 4, a nugget can be added to the diagonal of K to ensure that its condition number is smaller than a user-set threshold. However,

this same approach cannot be used on its own for K_∇ since it may require a significantly larger nugget value, which can significantly degrade the accuracy of the surrogate [3]. The previous methods that have been used to help alleviate the ill-conditioning problem of K_∇ are not always sufficient, and a constraint on the condition number may still be required in the optimization of the marginal log-likelihood [14]

$$\bar{\boldsymbol{\theta}}(\mathsf{X};\eta_{\mathsf{K}_\nabla}) = \underset{\boldsymbol{\theta}}{\operatorname{argmax}}\ \ln(L(\boldsymbol{\theta};\mathsf{X},\eta_{\mathsf{K}_\nabla})) \quad \text{such that } \kappa(\mathsf{K}_\nabla(\boldsymbol{\theta};\mathsf{X})+\eta_{\mathsf{K}_\nabla}\mathsf{I}) \leq \kappa_{\max}. \tag{12}$$

The constraint on the condition number can severely limit the selection of the hyperparameters and this can impact the effectiveness of the GP to model the function of interest, as will be demonstrated in Section 10. An efficient way of solving Eq. (12) is with a gradient-based optimizer [26,23,14]. However, the marginal log-likelihood is often multimodal, which creates the risk of finding a local minimum [21]. As such, if a gradient-based optimizer is used, several starting solutions should be used to avoid finding a local optimal with a small marginal likelihood.

4 The role of the nugget

The nugget is a positive scalar that is added to the diagonal of the covariance matrix to help alleviate the ill-conditioning problem. We derive bounds for η_{K} and η_{K_∇} to ensure $\kappa(\mathsf{K}(\boldsymbol{\theta}) + \eta_{\mathsf{K}}\mathsf{I}) \leq \kappa_{\max}$ and $\kappa(\mathsf{K}_\nabla(\boldsymbol{\theta}) + \eta_{\mathsf{K}_\nabla}\mathsf{I}) \leq \kappa_{\max}$, respectively. In the derivations we use only the trace of K and K_∇ in addition to the symmetric positive definite property of these matrices. The eigenvalues are ordered such that $\lambda_{\min} = \lambda_1 \leq \lambda_2 \leq \ldots \leq \lambda_{n_\lambda} = \lambda_{\max}$, where n_λ is the number of eigenvalues. For K we have $n_\lambda = n_x$ and for K_∇ we have $n_\lambda = n_x(d+1)$. The traces for K and K_∇ are

$$\operatorname{tr}(\mathsf{K}) = n_x \tag{13}$$

$$\operatorname{tr}(\mathsf{K}_\nabla) = n_x(1 + 2\boldsymbol{\theta}^T\mathbf{1}). \tag{14}$$

The impact of adding η to the diagonal of a matrix and its use to bound the condition number is considered in the following lemma.

Lemma 1 *For the condition number defined using the Euclidean norm and a symmetric positive definite matrix* A*, a lower bound for* η *that ensures that* $\kappa(\mathsf{A}+\eta\mathsf{I}) \leq \kappa_{\max}$*, where* $\kappa_{\max}$ *is a user-set upper bound on the condition number, is*

$$\eta \geq \frac{\lambda_{max}}{\kappa_{\max} - 1}. \tag{15}$$

Proof Consider the following relations

$$\kappa(\mathsf{A}+\eta\mathsf{I}) = \frac{\lambda_{\max}+\eta}{\lambda_{\min}+\eta} < \frac{\lambda_{\max}}{\eta} + 1 \leq \kappa_{\max},$$

where all the eigenvalues are increased by η since it is added to the diagonal of A, which has real eigenvalues since it is symmetric. We recover Eq. (15) by solving the last inequality for η.

For a positive definite matrix we have $\lambda_{\max}(\mathsf{A}) < \operatorname{tr}(\mathsf{A})$ since the sum of a matrix's eigenvalues is equal to its trace. From Lemma 1 and Eqs. (13) and (14) we can thus ensure that $\kappa(\mathsf{K}+\eta_{\mathsf{K}}) \leq \kappa_{\max}$ and $\kappa(\mathsf{K}_\nabla+\eta_{\mathsf{K}_\nabla}) \leq \kappa_{\max}$ with

$$\eta_{\mathsf{K}} = \frac{n_x}{\kappa_{\max}-1} \tag{16}$$

$$\eta_{\mathsf{K}_\nabla} = \frac{n_x(1+2\boldsymbol{\theta}^T\mathbf{1})}{\kappa_{\max}-1}. \tag{17}$$

From Eq. (16), η_{K} only depends on n_x and $\kappa_{\max}$. Meanwhile, from Eq. (17), η_{K_∇} depends on n_x, $\kappa_{\max}$, and also $\boldsymbol{\theta}$. As such, it is not possible to have a moderate value of η_{K_∇} to ensure $\kappa\left(\mathsf{K}_\nabla(\theta)+\eta_{\mathsf{K}_\nabla}\mathsf{I}\right) \leq \kappa_{\max}$ without restricting $\boldsymbol{\theta}$. In Sections 8 and 9 additional information on the structure of K_∇ is used to derive a smaller value of η_{K_∇} that ensures $\kappa(\mathsf{K}_\nabla+\eta_{\mathsf{K}_\nabla}\mathsf{I}) \leq \kappa_{\max}$. Those sections use Geshgorin's circle theorem to bound the eigenvalues of K_∇, as is demonstrated for K in the following section.

5 The ill-conditioning problem

In this paper the focus is on the Gaussian kernel. However, various other kernels are also known to suffer from ill-conditioned covariance matrices [1]. In this section we highlight the ill-conditioning of the gradient-enhanced covariance matrices that use the Gaussian, rational quadratic, and Matérn kernels. The rational quadratic kernel is given by

$$k(\boldsymbol{x},\boldsymbol{y}) = \left(1+\frac{1}{\alpha}\sum_{i=1}^{d}\theta_i(x_i-y_i)^2\right)^{-\alpha}, \tag{18}$$

where $\alpha > 0$ is a hyperparameter that is set by maximizing the marginal log-likelihood from Eq. (12). The Matérn kernel can be parametrized with a hyperparameter ν and is most commonly used with $\nu \in \{\frac{1}{2}, \frac{3}{2}, \frac{5}{2}\}$. We consider the Matérn kernel with $\nu = \frac{5}{2}$ since it is twice continuously differentiable [16], and can thus be used by a gradient-enhanced GP

$$k(\boldsymbol{x},\boldsymbol{y}) = \left(1+\sqrt{5}\zeta+\frac{5\zeta^2}{3}\right)e^{-\sqrt{5}\zeta}, \tag{19}$$

where $\zeta(\boldsymbol{x},\boldsymbol{y}) = \sqrt{\sum_{i=1}^{d}\theta_i(x_i-y_i)^2}$. The Gaussian kernel can be recovered from the Matérn and rational quadratic kernels with $\nu \to \infty$ and $\alpha \to \infty$, respectively [16].

The condition numbers for the gradient-enhanced covariance matrices using the Gaussian, rational quadratic, and Matérn $\frac{5}{2}$ kernels are compared in

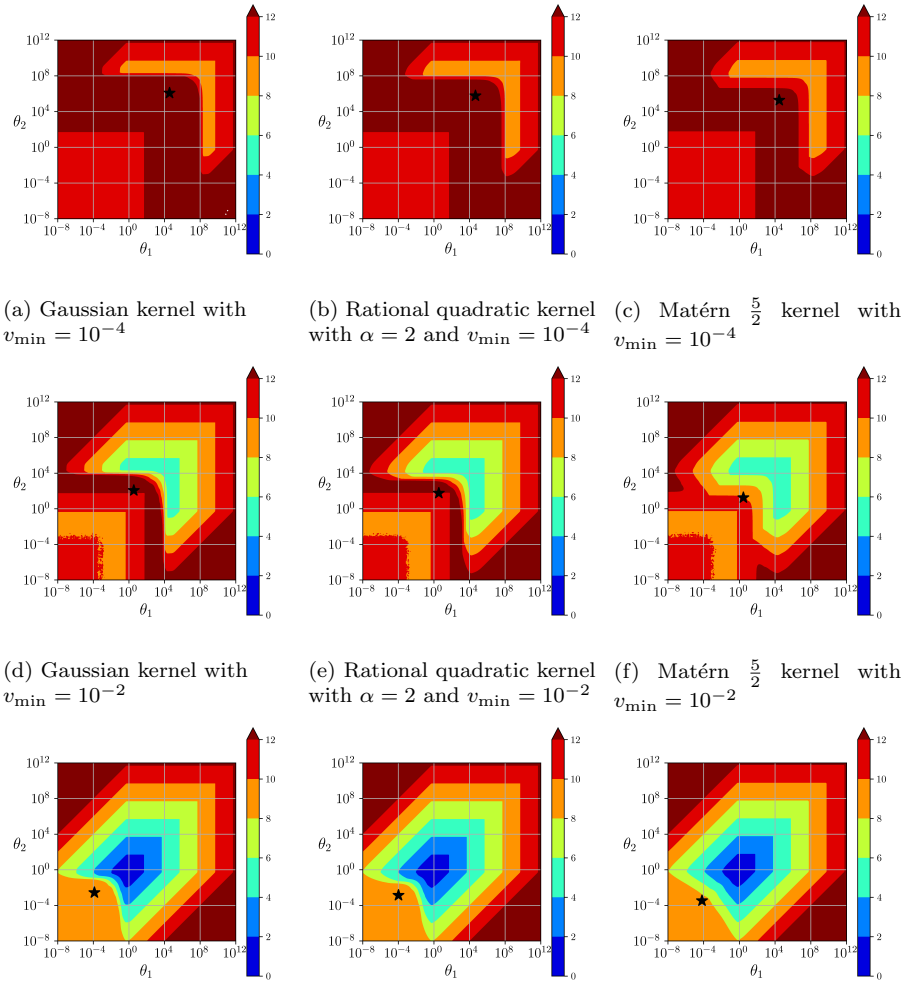

(a) Gaussian kernel with $v_{\min} = 10^{-4}$

(b) Rational quadratic kernel with $\alpha = 2$ and $v_{\min} = 10^{-4}$

(c) Matérn $\frac{5}{2}$ kernel with $v_{\min} = 10^{-4}$

(d) Gaussian kernel with $v_{\min} = 10^{-2}$

(e) Rational quadratic kernel with $\alpha = 2$ and $v_{\min} = 10^{-2}$

(f) Matérn $\frac{5}{2}$ kernel with $v_{\min} = 10^{-2}$

(g) Gaussian kernel with $v_{\min} = 2\sqrt{2}$

(h) Rational quadratic kernel with $\alpha = 2$ and $v_{\min} = 2\sqrt{2}$

(i) Matérn $\frac{5}{2}$ kernel with $v_{\min} = 2\sqrt{2}$

Fig. 1: Comparing $\kappa\left(\mathsf{K}_\nabla(\boldsymbol{\theta}) + \eta_{\mathsf{K}_\nabla}\mathsf{I}\right)$ for the Gaussian, Matérn $\frac{5}{2}$, and rational quadratic kernels for $d = 2$, $n_x = 10$, and $\eta_{\mathsf{K}_\nabla} = \eta_{\mathsf{K}} = 10^{-9}$ from Eq. (16). The star marker indicates where the marginal likelihood from Eq. (12) is maximized and red regions indicate where $\kappa\left(\mathsf{K}_\nabla(\boldsymbol{\theta}) + \eta_{\mathsf{K}_\nabla}\mathsf{I}\right) \geq \kappa_{\max} = 10^{10}$.

Fig. 1. The set of data points was created with a Latin hypercube sampling and $n_x = 10$. An isotropic rescaling was then used to change the minimum Euclidean distance $v_{\min}$ between data points in order to evaluate its impact on the condition number of the gradient-enhanced covariance matrix. While the function of interest does not modify the condition number of the gradient-

enhanced covariance matrix, it does impact the solution that maximizes the marginal log-likelihood from Eq. (12). For our function of interest we use the Rosenbrock function

$$f(\boldsymbol{x}) = \sum_{i=1}^{d-1} \left[a \left(x^{(i+1)} - \left(x^{(i)} \right)^2 \right) + \left(1 - x^{(i)} \right)^2 \right] \tag{20}$$

with $a = 10$ and $d = 2$.

For the gradient-free case there are various factors that have been identified that contribute to an ill-conditioned covariance matrix, including when the characteristic lengths tend to zero [4]. However, as can be seen in Fig. 1, the gradient-enhanced covariance matrix can become ill-conditioned not only when the characteristic lengths are small, but also when they are large.

The subfigures in the top row of Fig. 1, i.e. Figs. 1a, 1b, and 1c, are for the Gaussian, rational quadratic, and Matérn $\frac{5}{2}$ kernels, respectively, with $v_{\min} = 10^{-4}$. The location where the marginal log-likelihood is maximized, which is indicated by the star marker, corresponds with a gradient-enhanced covariance matrix with a condition number greater than $\kappa_{\max}$ for all three kernels. For the second row of subfigures in Fig. 1, i.e. Figs. 1d, 1e, and 1f, $v_{\min}$ is increased to 10^{-2} and the region in the hyperparameter space where $\kappa\left(\mathsf{K}_\nabla(\boldsymbol{\theta}) + \eta_{\mathsf{K}_\nabla}\mathsf{I}\right) \geq \kappa_{\max} = 10^{10}$ is reduced significantly. Once again, the star markers for all three kernels remain in the red region, indicating the condition number is larger than $\kappa_{\max} = 10^{10}$. Finally, in the last row of Fig. 1, i.e. Figs. 1g, 1h, and 1i, we have $v_{\min} = 2\sqrt{2}$. In this case the star marker for all three kernels corresponds with a condition number that is smaller than $\kappa_{\max} = 10^{10}$.

It is clear from Fig. 1 that the condition number of the gradient-enhanced covariance matrix using the Gaussian kernel is the largest, followed closely by the rational quadratic kernel with $\alpha = 2$, while the Matérn $\frac{5}{2}$ kernel has the smallest condition number for all three cases of $v_{\min}$. Additionally, for all three kernels the condition number of the gradient-enhanced covariance matrix is inversely related to $v_{\min}$. This trend is proved for the Gaussian kernel and used in Section 8 to demonstrate that having $v_{\min} \geq 2\sqrt{d}$ ensures that $\kappa\left(\mathsf{K}_\nabla(\boldsymbol{\theta}) + \eta_{\mathsf{K}_\nabla}\mathsf{I}\right) \leq \kappa_{\max}$ for the Gaussian kernel under mild conditions. While the proofs are specific to the Gaussian kernel, it is clear from Fig. 1 that with $v_{\min} = 2\sqrt{d}$, both the rational quadratic $\alpha = 2$ and Matérn $\frac{5}{2}$ kernels have $\kappa\left(\mathsf{K}_\nabla(\boldsymbol{\theta}) + \eta_{\mathsf{K}_\nabla}\mathsf{I}\right) \leq \kappa_{\max}$ at the star marker. The results from this paper can thus be applied to other kernels to alleviate the ill-conditioning problem of their gradient-enhanced covariance matrices.

6 Bounding $\kappa(\mathsf{K} + \eta_{\mathsf{K}}\mathsf{I})$ with Geshgorin's circle theorem

Gershgorin's circle theorem bounds the location of a matrix's eigenvalues in the complex plane. The eigenvalues are further restricted to the real axis since

K and K_∇ are symmetric. With Gershgorin's circle theorem we get the following lower bound for the smallest eigenvalue and upper bound for the largest eigenvalue of a matrix A with

$$\lambda_{\min}(\mathsf{A}) \geq \min_i \left(\mathsf{A}_{ii} - r_i\right) \geq \min_i \left(\mathsf{A}_{ii} - u_{r_i}\right) = \ell_{\lambda_{\min}}(\mathsf{A}) \tag{21}$$

$$\lambda_{\max}(\mathsf{A}) \leq \max_i \left(\mathsf{A}_{ii} + r_i\right) \leq \max_i \left(\mathsf{A}_{ii} + u_{r_i}\right) = u_{\lambda_{\max}}(\mathsf{A}), \tag{22}$$

where $r_i = \sum_{j \neq i} |\mathsf{A}_{ij}|$ and u_{r_i} is an upper bound on r_i. The bounds $\ell_{\lambda_{\min}}$ and $u_{\lambda_{\max}}$ represent the lower and upper bounds on the eigenvalues of a given matrix from the application of Gershgorin's circle theorem. Since the positive definite property of the matrix is not used, we may have $\ell_{\lambda_{\min}} < 0$. The condition number of a positive definite matrix based on the Euclidean norm can be bounded with

$$u_\kappa(\mathsf{A} + \eta) = \frac{u_{\lambda_{\max}}(\mathsf{A}) + \eta}{\max(0, \ell_{\lambda_{\min}}(\mathsf{A})) + \eta}. \tag{23}$$

All of the diagonal entries in K are one, which simplifies Eqs. (21) and (22) to

$$\ell_{\lambda_{\min}} = 1 - u_{r_\mathsf{K}} \tag{24}$$

$$u_{\lambda_{\max}} = 1 + u_{r_\mathsf{K}}, \tag{25}$$

where u_{r_K} is an upper bound on the sum of the off-diagonal entries of K that is considered in Proposition 1.

To simplify the derivation of u_{r_K} we consider the case of $\boldsymbol{\theta} = \theta\mathbf{1}$. This simplification reduces the number of hyperparameters in the analysis from d to one. This simplification is used both in this section as well as in Section 7 for the analysis of K_∇. In Section 10.4 an iterative non-isotropic rescaling method is introduced to ensure $\boldsymbol{\theta} = \theta\mathbf{1}$. Therefore, the simplification $\boldsymbol{\theta} = \theta\mathbf{1}$ does not limit the analysis of this section or the next one for K_∇. An upper bound on the sum of absolute values of the off-diagonal entries for K is considered in the next proposition.

Proposition 1 *The maximum sum of the off-diagonal entries for one row of* $\mathsf{K}(\boldsymbol{\theta})$ *when* $\boldsymbol{\theta} = \theta\mathbf{1}$ *is bounded from above by* $\max_j \sum_{i=1, i\neq j}^{n_x} \mathsf{K}_{ij} \leq u_{r_\mathsf{K}}$*, where*

$$u_{r_\mathsf{K}}(\theta; v_{min}, n_x) = (n_x - 1)e^{-\theta v_{min}^2}, \tag{26}$$

where v_{min} *is the shortest Euclidean distance between any two rows in the matrix* X*, i.e. between two evaluated points in the parameter space.*

Proof Eq. (5) provides the structure of the matrix K, which is used to derive the upper bound on the sum of the off-diagonal entries. When $\boldsymbol{\theta} = \theta\mathbf{1}$, the

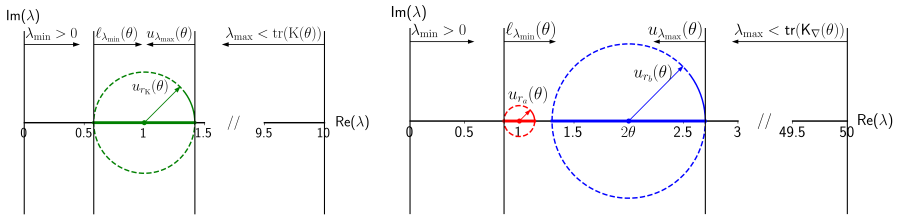

(a) K with $v_{\min} = 1.75$. (b) K_∇ with $v_{\min} = 2.5$.

Fig. 2: Bounds on the eigenvalues of the covariance matrices using Gershgorin's circle theorem for the case with $d = 2$, $n_x = 10$, and $\theta = 1$.

result is the same for any row considered and we thus arbitrarily select the j-th row of K

$$\begin{aligned} r_{\mathsf{K},j} &= \sum_{\substack{i=1 \\ i \neq j}}^{n_x} e^{-\sum_{m=1}^{d} \theta \left(x_j^{(m)} - x_i^{(m)} \right)^2} \\ &= \sum_{\substack{i=1 \\ i \neq k}}^{n_x} e^{-\theta \| x_j - x_i \|_2^2} \\ &\leq (n_x - 1) e^{-\theta v_{\min}^2}, \end{aligned}$$

which holds for all rows in K since $v_{\min} = \min_{i \neq j} \| x_j - x_i \|_2$.

From Eq. (26) it is clear that $v_{\min}$ plays an important role in bounding the condition number of K. The same is true for bounding the condition number of K_∇, as shown in Section 7 below. Given a matrix X_{init} with $v_{\min,\text{init}} > 0$ as the minimum Euclidean distance between all rows, i.e. evaluated points in the parameter space, we can scale the data isotropically with

$$\mathsf{X} = \tau \, \mathsf{X}_{\text{init}} \tag{27}$$

$$\mathsf{F}_\nabla = \frac{1}{\tau} \mathsf{F}_{\nabla,\text{init}}, \tag{28}$$

where $\tau = \frac{v_{\min,\text{set}}}{v_{\min,\text{init}}}$, and $v_{\min,\text{set}}$ is the new minimum Euclidean distance between rows in X.

Fig. 2a shows the bounds on $\lambda_{\min}$ and $\lambda_{\max}$ from Eqs. (24) and (25) for $v_{\min} = 1.75$, $\theta = 1$, $d = 2$, and $n_x = 10$. The bounds use Gershgorin's circle theorem, which bounds the eigenvalues in the complex plane, but the eigenvalues are further limited to the solid green line on the real axis since K is symmetric. For the case plotted in Fig. 2a, it is clear that the bound on $\lambda_{\max}$ from Eq. (25) and Gershgorin's circle theorem is significantly tighter than simply using the trace of K from Eq. (13).

Fig. 3a shows the minimum and maximum eigenvalues of K for $d = 2$, $n_x = 10$, $v_{\min} = 2\sqrt{2}$, and $\eta_{\mathsf{K}} = 10^{-9}$ as a function of θ along with its bounds

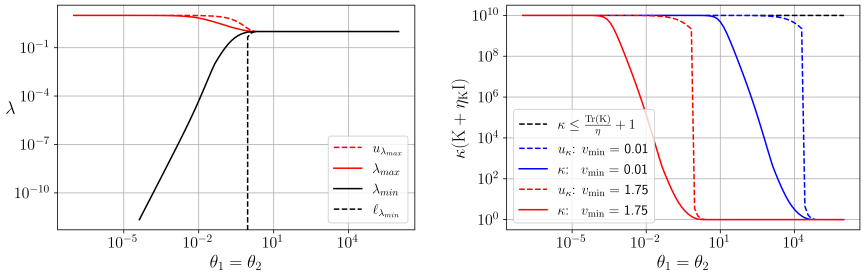

(a) Min and max eigenvalues of K along with their respective bounds from Eqs. (24) and (25) for $v_{\min} = 1.75$.

(b) The condition number of $\mathsf{K} + \eta_\mathsf{K}\mathsf{I}$ along with its upper bound from Eq. (23).

Fig. 3: Case with $d = 2$, $n_x = 10$, and $\eta_\mathsf{K} = 10^{-9}$ for the gradient-free covariance matrix K.

using Eqs. (24) and (25). Fig. 3b compares the condition number along with its derived upper bound from Eq. (23) for two covariance matrices. The covariance matrices are both constructed from a single matrix X rescaled isotropically using Eq. (27) to have different minimum Euclidean distances between its rows. From Fig. 3b, we see that the impact of increasing $v_{\min}$ is to shift the plots of $\lambda_{\min}(\theta)$, $\lambda_{\max}(\theta)$, and $\kappa(\mathsf{K}(\theta) + \eta_\mathsf{K}\mathsf{I})$ to the right. While changing $v_{\min}$ does not impact the maximum value of $\kappa\left(\mathsf{K} + \eta_\mathsf{K}\mathsf{I}\right)$, it does impact the maximum of $\kappa\left(\mathsf{K}_\nabla + \eta_{\mathsf{K}_\nabla}\mathsf{I}\right)$, as is shown in Section 7.

7 Relations for bounding the condition number of $\mathsf{K}_\nabla + \eta_{\mathsf{K}_\nabla}\mathsf{I}$

7.1 Bounding the sum of the off-diagonal entries of K_∇

As was done in Section 6, the analysis in this section uses the simplification $\boldsymbol{\theta} = \theta\mathbf{1}$. In Section 10.4 it is demonstrated that non-isotropic rescaling of X and F_∇ can be used to ensure the solution to Eq. (12) also satisfies $\boldsymbol{\theta} = \theta\mathbf{1}$. As such, the analysis in this section is applicable even when the solution to Eq. (12) prior to the rescaling of X and F_∇ does not satisfy $\boldsymbol{\theta} = \theta\mathbf{1}$.

The matrix K_∇ has different values along its diagonal and the matrix structure is different for the first n_x rows and the remaining $d \cdot n_x$ rows. The two following propositions provide upper bounds on the sum of the absolute values of the off-diagonal entries of K_∇.

Proposition 2 *The sum of the absolute values of the off-diagonal entries for any of the first n_x rows of $\mathsf{K}_\nabla(\boldsymbol{\theta})$ when $\boldsymbol{\theta} = \theta\mathbf{1}$ is bounded by*

$$u_{r_a}(\theta, v_a(\theta; v_{min}, d); d, n_x) = (n_x - 1)\left(1 + 2\theta\sqrt{d}v_a\right)e^{-\theta v_a^2}, \tag{29}$$

where

$$v_a(\theta; v_{min}, d) = \max\left(v_{min}, v_a^*(\theta; d)\right) \tag{30}$$
$$v_a^*(\theta; d) = \underset{v}{\operatorname{argmax}}\, u_{r_a}(\theta, v); d, n_x). \tag{31}$$

Proof The structure of K_∇ is provided by Eq. (8). For $\boldsymbol{\theta} = \theta\mathbf{1}$, the derivation is the same for any of the first n_x rows and we thus arbitrarily consider the a-th row of K_∇, where $1 \leq a \leq n_x$

$$\begin{aligned}
r_a\left(\theta; \mathsf{X}\right) &= \sum_{\substack{i=1 \\ i\neq a}}^{n_x} e^{-\theta\|\boldsymbol{x}_a - \boldsymbol{x}_i\|_2^2} + \sum_{j=1}^{d}\sum_{\substack{i=1 \\ i\neq a}}^{n_x} 2\theta|x_a^{(j)} - x_i^{(j)}|e^{-\theta\|\boldsymbol{x}_a - \boldsymbol{x}_i\|_2^2} \\
&= \sum_{\substack{i=1 \\ i\neq a}}^{n_x} \left(1 + 2\theta\sum_{j=1}^{d}|x_a^{(j)} - x_i^{(j)}|\right) e^{-\theta\|\boldsymbol{x}_a - \boldsymbol{x}_i\|_2^2} \\
&\leq \sum_{\substack{i=1 \\ i\neq a}}^{n_x} \left(1 + 2\theta\sqrt{d}\|\boldsymbol{x}_a - \boldsymbol{x}_i\|_2\right) e^{-\theta\|\boldsymbol{x}_a - \boldsymbol{x}_i\|_2^2} \\
&\leq (n_x - 1)\left(1 + 2\theta\sqrt{d}v_a\right) e^{-\theta v_a^2},
\end{aligned}$$

where $\sum_{j=1}^{d}|x_i^{(j)} - x_j^{(j)}| = \|x_i^{(j)} - x_j^{(j)}\|_1 \leq \sqrt{d}\|x_i^{(j)} - x_j^{(j)}\|_2$. The parameter v_a is selected to ensure u_{r_a} is an upper bound for r_a and is thus given by Eq. (30).

Proposition 3 *The sum of the absolute values of the off-diagonal entries for any of the last $d \cdot n_x$ rows of $\mathsf{K}_\nabla(\boldsymbol{\theta})$ when $\boldsymbol{\theta} = \theta\mathbf{1}$ is bounded by*

$$u_{r_b}(\theta, v_b(\theta; v_{min}, d); d, n_x) = 2\theta v_b(n_x - 1)\left(1 + 2\theta\sqrt{d}\, v_b\right) e^{-\theta v_b^2}, \tag{32}$$

where

$$v_b(\theta; v_{min}, d) = \max\left(v_{min}, v_b^*(\theta; d)\right) \tag{33}$$
$$v_b^*(\theta; d) = \underset{v}{\operatorname{argmax}}\, u_{r_b}(\theta, v; d, n_x). \tag{34}$$

Proof We consider the b-th row of K_∇, where $b = k_1 n_x + k_2$, $1 \leq k_1 \leq d$, $1 \leq k_2 \leq n_x$, and we follow a similar approach to the one taken to prove

Proposition 2

$$
\begin{aligned}
r_b(\theta;\mathsf{X}) &= \sum_{i=1}^{n_x} 2\theta|x_{k_2}^{(k_1)} - x_i^{(k_1)}|e^{-\theta\|\boldsymbol{x}_{k_2}-\boldsymbol{x}_i\|_2^2} \\
&\quad + \sum_{j=1}^{d}\sum_{i=1}^{n_x} 4\theta^2|x_{k_2}^{(k_1)} - x_i^{(k_1)}||x_{k_2}^{(j)} - x_i^{(j)}|e^{-\theta\|\boldsymbol{x}_{k_2}-\boldsymbol{x}_i\|_2^2} \\
&= \sum_{i=1}^{n_x}\left[2\theta|x_{k_2}^{(k_1)} - x_i^{(k_1)}|\left(1 + 2\theta\sum_{j=1}^{d}|x_{k_2}^{(j)} - x_i^{(j)}|\right)\right] e^{-\theta\|\boldsymbol{x}_{k_2}-\boldsymbol{x}_i\|_2^2} \\
&\leq \sum_{i=1}^{n_x}\left[2\theta\|\boldsymbol{x}_{k_2} - \boldsymbol{x}_i\|_2\left(1 + 2\theta\sqrt{d}\|\boldsymbol{x}_{k_2} - \boldsymbol{x}_i\|_2\right)\right] e^{-\theta\|\boldsymbol{x}_{k_2}-\boldsymbol{x}_i\|_2^2} \\
&\leq 2\theta v_b(n_x - 1)\left(1 + 2\theta\sqrt{d}\, v_b\right) e^{-\theta v_b^2},
\end{aligned}
$$

where the relation $|x_{k_2}^{(k_1)} - x_i^{(k_1)}| \leq \|\boldsymbol{x}_{k_2} - \boldsymbol{x}_i\|_2$ was used. To ensure r_b is bounded from above, the parameter v_b is given by Eq. (33).

As a result of Propositions 2 and 3 and Eqs. (21) and (22), the eigenvalues of K_∇ are bounded from below and above by

$$\ell_{\lambda_{\min}}(\theta; v_{\min}, d, n_x) = \min(1 - u_{r_a},\, 2\theta - u_{r_b}) \tag{35}$$

$$u_{\lambda_{\max}}(\theta; v_{\min}, d, n_x) = \max(1 + u_{r_a}, 2\theta + u_{r_b}). \tag{36}$$

The application of Eqs. (35) and (36) is shown in Fig. 2b for the case with $d = 2$, $n_x = 10$, and $\theta = 1$. For the case in Fig. 2b, the bounds provided on $\lambda_{\min}$ and $\lambda_{\max}$ from Eqs. (35) and (36) are tighter than the previous bounds, which were $\lambda_{\min} > 0$ and $\lambda_{\max} < \mathrm{tr}\,(\mathsf{K}_\nabla)$.

The upper bounds $u_{r_a}(\theta, v_a)$ and $u_{r_b}(\theta, v_b)$ from Eqs. (29) and (32) are plotted as a function of v_a and v_b, respectively, in Fig. 4 with $\theta = \frac{1}{2}$, $d = 10$, and $n_x = 4$. The shaded cyan region represents the range of Euclidean distances between two rows in the matrix X. As will be explained in Section 7.4, only the minimum Euclidean distance, i.e. $v_{\min}$, is important for bounding the condition number of K_∇, which is why $v_{\max}$ is omitted from Eqs. (30) and (33). For the case shown in Fig. 4, there is a unique maximum for both $u_{r_a}(v_a)$ and $u_{r_b}(v_b)$. In Sections 7.2 and 7.3 it is proven that there is always a unique maximum for $d \in \mathbb{Z}^+$, $n_x \in \mathbb{Z}^+ \setminus 1$, and $v_{\min} > 0$.

Fig. 5 plots $u_{r_a}(\theta, v_a(\theta))$ and $u_{r_b}(\theta, v_b(\theta))$ for $n_x = 4$, $d = 10$, and $v_{\min} = \sqrt{2}$. In Sections 7.2 and 7.3 the functions $u_{r_a}^*(v_{\min}, d, n_x)$ and $u_{r_a}^*(v_{\min}, d, n_x)$, i.e. the maximum of u_{r_a} and u_{r_b}, respectively, are derived. This is then used in Sections 8 and 9 to derive values of $v_{\min}$ and η_{K_∇} to ensure $\kappa\left(\mathsf{K}_\nabla + \eta_{\mathsf{K}_\nabla}\mathsf{I}\right) \leq \kappa_{\max}$.

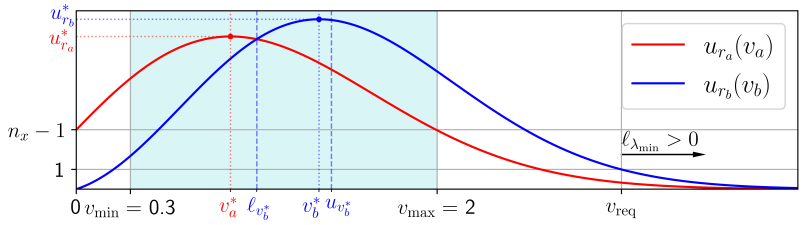

Fig. 4: The dependence of the upper bounds u_{r_a} and u_{r_b} from Eqs. (29) and (32), respectively, on the distance parameter v for the case with $n_x = 4$, $d = 10$, and $\theta = \frac{1}{2}$.

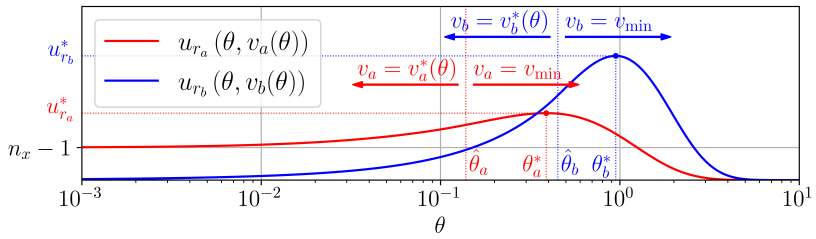

Fig. 5: Upper bounds $u_{r_a}(\theta, v_a(\theta))$ and $u_{r_b}(\theta, v_b(\theta))$ from Eqs. (29) and (32), respectively, for $n_x = 4$, $d = 10$, and $v_{\min} = \sqrt{2}$.

7.2 Maximum of $u_{r_a}(\theta, v_a(\theta))$

In this subsection the maximum of $u_{r_a}(\theta, v_a(\theta; v_{\min}, d); d, n_x)$ is derived for $\theta > 0$, $v_{\min} > 0$, $d \in \mathbb{Z}^+$, and $n_x \in \mathbb{Z}^+$. The maximum of $u_{r_a}(\theta, v_a(\theta))$ as a function of θ is considered in the next proposition.

Proposition 4 *For $\theta \geq 0$, $d \in \mathbb{Z}^+$, and $n_x \in \mathbb{Z}^+$, the maximum of $u_{r_a}(\theta, v_a(\theta))$ is at*

$$\theta^*_a(v_a, d) = \max\left(0, \frac{2\sqrt{d} - v_a}{2\sqrt{d}v_a^2}\right). \tag{37}$$

Proof We find the maximum of $u_{r_a}(\theta, v_a(\theta))$ by using the chain rule

$$\frac{Du_{r_a}(\theta, v_a(\theta))}{D\theta} = \frac{\partial u_{r_a}}{\partial \theta} + \begin{cases} \cancel{\frac{\partial u_{r_a}}{\partial v_a}}^{0} \frac{\partial v_a}{\partial \theta} & \text{if } v_a(\theta) = v^*_a(\theta) > v_{\min} \\ \frac{\partial u_{r_a}}{\partial v_a} \cancel{\frac{\partial v_a}{\partial \theta}}^{0} & \text{if } v_a(\theta) = v_{\min}, \end{cases}$$

where $\frac{\partial u_{r_a}}{\partial v_a} = 0$ when $v_a(\theta) = v^*_a(\theta)$ since v^*_a is the critical point that maximizes $u_{r_a}(v_a)$. This was verified by checking the second-order optimality condition, which is omitted for conciseness. We can thus find the maximum of

$u_{r_a}(\theta, v_a(\theta))$ by finding the root of its partial derivative with respect to θ

$$\frac{\partial u_{r_a}}{\partial \theta} = (n_x - 1)\left(2\sqrt{d}v_a - v_a^2(1 + 2\sqrt{d}\theta v_a)\right)e^{-\theta v_a^2} = 0$$
$$\theta_a^* = \frac{2\sqrt{d} - v_a}{2\sqrt{d}v_a^2},$$

where we recover Eq. (37) by including a max function to ensure $\theta_a^* \geq 0$, which completes the proof.

In order to calculate θ_a^* from Eq. (37) we need to evaluate $v_a(\theta_a^*)$ from Eq. (30). At first it might appear that we have an implicit equation but it will be proven in this subsection that $v_a(\theta_a^*) = v_{\min}$. From Eq. (30), v_a is simply the maximum of $v_{\min}$ and v_a^*, where the latter is provided by the following proposition.

Proposition 5 *For $v_a > 0$, $d \in \mathbb{Z}^+$, $n_x \in \mathbb{Z}^+$, and $\theta > 0$, the function $u_{r_a}(v_a)$ is maximized at $v_a = v_a^*$, where*

$$v_a^*(\theta; d) = \frac{-1 + \sqrt{1 + 8d\theta}}{4\theta\sqrt{d}}. \tag{38}$$

Proof We demonstrate there is a unique maximum of $u_{r_a}(v_a)$ for $v_a > 0$ by calculating its derivative

$$\frac{\partial u_{r_a}}{\partial v_a} = -2\theta(n_x - 1)\left[2\theta\sqrt{d}v_a^2 + v_a - \sqrt{d}\right]e^{-\theta v_a^2}. \tag{39}$$

The positive root for the quadratic equation in square brackets is given by Eq. (38). For $v_a > v_a^*$, the quadratic in Eq. (39) is positive and thus $\frac{\partial u_{r_a}}{\partial v_a} < 0$. On the other hand, for $0 < v_a < v_a^*$ it is clear that $\frac{\partial u_{r_a}}{\partial v_a} > 0$. Therefore, the critical point $v_a = v_a^*$ is the maximum of $u_{r_a}(v_a)$.

The following proposition considers the trends of $v_a^*(\theta; d)$ with respect to θ and d, which are required to prove that at $\theta = \theta_a^*$ we have $v_a^* < v_{\min}$ and thus $v_a(\theta_a^*) = v_{\min}$.

Proposition 6 *For $d \in \mathbb{Z}^+$ and $\theta > 0$ the function $v_a^*(\theta; d)$ is monotonically increasing with respect to d, monotonically decreasing with respect to θ, and is bounded from above by*

$$u_{v_a^*} = \min\left(\sqrt{d}, \frac{1}{\sqrt{2\theta}}\right). \tag{40}$$

Proof The proof can be found in Section 12.1.

The following proposition proves that $v_a(\theta_a^*) = v_{\min}$, which is needed to evaluate θ_a^* from Eq. (37).

Proposition 7 *For $d \in \mathbb{Z}^+$, $v_{min} > 0$, and $\theta \geq \hat{\theta}_a$, which includes $\theta \geq \theta_a^*$, we have $v_a(\theta) = v_{min}$, where*

$$\hat{\theta}_a(v_{min}, d) = \frac{\sqrt{d} - v_{min}}{2\sqrt{d}\, v_{min}^2}. \tag{41}$$

Proof We begin by solving for $\hat{\theta}_a(v_{\min}, d)$, which is the value of θ at which we have $v_a(\theta) = v_a^*(\theta) = v_{\min}$

$$\begin{aligned} v_{\min} &= \frac{-1 + \sqrt{1 + 8d\hat{\theta}_a}}{4\hat{\theta}_a\sqrt{d}} \\ 16v_{\min}^2 d\hat{\theta}_a^2 + 8v_{\min}\sqrt{d}\hat{\theta}_a + 1 &= 1 + 8d\hat{\theta}_a, \end{aligned}$$

where we recover Eq. (41) by isolating for $\hat{\theta}_a$ in the last equation. From Proposition 6 we know that $v_a^*(\theta)$ is monotonically decreasing with respect to θ. Therefore, for $\theta > \hat{\theta}_a$ we have $v_a^*(\theta) < v_{\min}$ and thus from Eq. (30) it follows that $v_a(\theta > \hat{\theta}_a) = v_{\min}$. From Eqs. (37) and (41) we have the relation $\theta_a^* = \frac{2\sqrt{d} - v_{\min}}{2\sqrt{d}} > \frac{\sqrt{d} - v_{\min}}{2\sqrt{d}} = \hat{\theta}_a$. We thus have $v_a(\theta \geq \theta_a^*) = v_{\min}$, which completes the proof.

As a result of Propositions 4 and 7 we know that the maximum of $u_{r_a}(\theta, v_a; d, n_x)$ is at $\theta = \theta_a^*$ and $v_a = v_{\min}$. For $0 < v_{\min} \leq 2\sqrt{d}$ we thus have

$$\begin{aligned} u_{r_a}^*(v_{\min}, d, n_x) &= u_{r_a}(\theta_a^*(v_{\min}), v_{\min}; d, n_x) \\ &= (n_x - 1)\left(1 + 2\sqrt{d}\, v_{\min}\left(\frac{2\sqrt{d} - v_{\min}}{2\sqrt{d}\, v_{\min}^2}\right)\right) e^{-\left(\frac{2\sqrt{d} - v_{\min}}{2\sqrt{d}\, v_{\min}^2}\right) v_{\min}^2} \\ &= (n_x - 1)\frac{2\sqrt{d}}{v_{\min}} e^{\frac{v_{\min} - 2\sqrt{d}}{2\sqrt{d}}}. \end{aligned} \tag{42}$$

Eq. (37) indicates that for $v_{\min} \geq 2\sqrt{d}$ we have $\theta_a^* = 0$ and it is straightforward to show that this gives $u_{r_a}^*(v_{\min}) = n_x - 1$.

7.3 Maximum of $u_{r_b}(\theta, v_b(\theta))$

A similar approach to the one taken in Section 7.2 is used to derive the maximum of $u_{r_b}(\theta, v_b(\theta; v_{\min}, d); d, n_x)$ for $\theta > 0$, $v_{\min} > 0$, $d \in \mathbb{Z}^+$, and $n_x \in \mathbb{Z}^+$. The following proposition considers the maximum of $u_{r_b}(\theta, v_b(\theta))$ as a function of θ.

Proposition 8 *The maximum of $u_{r_b}(\theta, v_b(\theta))$ for $d \in \mathbb{Z}^+$, $n_x \in \mathbb{Z}^+$, and $\theta > 0$ is at $\theta = \theta_b^*(v_{min}; d)$, where*

$$\theta_b^*(v_b, d) = \frac{4\sqrt{d} + \sqrt{v_b^2 + 16d} - v_b}{4\sqrt{d}v_b^2}. \tag{43}$$

Proof The derivative of $u_{r_b}(\theta, v_b(\theta))$ with respect to θ is

$$\frac{Du_{r_b}(\theta, v_b(\theta))}{D\theta} = \frac{\partial u_{r_b}}{\partial \theta} + \begin{cases} \cancelto{0}{\frac{\partial u_{r_b}}{\partial v_b}} \frac{\partial v_b}{\partial \theta} & \text{if } v_b(\theta) = v_b^*(\theta) > v_{\min} \\ \frac{\partial u_{r_b}}{\partial v_b} \cancelto{0}{\frac{\partial v_b}{\partial \theta}} & \text{if } v_b(\theta) = v_{\min} \end{cases}$$

$$= -2v(n_x - 1)\left[2\sqrt{d}v_b^3\theta^2 + v_b(v_b - 4\sqrt{d})\theta - 1\right] e^{-\theta v_b^2} = 0,$$

where Eq. (43) is recovered by keeping the positive root of the quadratic equation for θ. It is straightforward to verify that θ_b^* from Eq. (43) satisfies the second-order optimality condition and is thus the critical value that maximizes $u_{r_b}(\theta, v_b(\theta))$.

Similar to Section 7.3, the remaining proofs in this subsection prove that $v_b(\theta_b^*) = v_{\min}$, which makes Eq. (43) an explicit equation. From Eq. (33), v_b depends on v_b^*, which is provided by the following proposition.

Proposition 9 *For $v_b > 0$, $\theta > 0$, $d \in \mathbb{Z}^+$, and $n_x \in \mathbb{Z}^+$, the function $u_{r_b}(v_b)$ is quasiconcave and its maximum is at*

$$v_b^*(\theta; d) = \frac{\sqrt{12d\theta + 1}}{3\theta\sqrt{d}} \cos\left(\frac{1}{3}\cos^{-1}\left(\frac{9d\theta - 1}{(12d\theta + 1)^{\frac{3}{2}}}\right)\right) - \frac{1}{6\theta\sqrt{d}}. \tag{44}$$

Proof The proof can be found in Section 12.2.

Using Eq. (44) in the analysis of later sections is cumbersome since it is a non-polynomial equation. The analysis is simplified with the lower and upper bounds for v_b^* that are presented in the following lemma.

Lemma 2 *For $d \in \mathbb{Z}^+$ and $\theta > 0$ we have $\ell_{v_b^*}(\theta) < v_b^*(\theta; d) < u_{v_b^*}(\theta)$, where*

$$\ell_{v_b^*}(\theta) = \frac{1}{\sqrt{2\theta}} \tag{45}$$

$$u_{v_b^*}(\theta) = \frac{1}{\sqrt{\theta}}. \tag{46}$$

Proof The proof can be found in Section 12.3.

The value at which we have $v_b(\theta) = v_b^*(\theta) = v_{\min}$ is $\theta = \hat{\theta}_b$. Solving for $\hat{\theta}_b$ requires solving a transcendental equation. However, this can be avoided by using the lower and upper bounds on $\hat{\theta}_b$ from the following lemma.

Lemma 3 *The value $\hat{\theta}_b$ at which we have $v_b(\hat{\theta}_b) = v_b^*(\hat{\theta}_b) = v_{min} > 0$ is bounded by $\ell_{\hat{\theta}_b}(v_{min}) < \hat{\theta}_b(v_{min}) < u_{\hat{\theta}_b}(v_{min})$, where*

$$\ell_{\hat{\theta}_b}(v_{min}) = \frac{1}{2v_{min}^2} \tag{47}$$

$$u_{\hat{\theta}_b}(v_{min}) = \frac{1}{v_{min}^2}. \tag{48}$$

Proof The bounds $\ell_{v_b^*}(\theta)$ and $u_{v_b^*}(\theta)$, which are given by Eqs. (45) and (46), respectively, are monotonically decreasing with respect to θ. Therefore, we can derive lower and upper bounds for $\hat{\theta}_b$ by isolating for θ in $\ell_{v_b^*}(\theta) = v_{\min}$ and $u_{v_b^*}(\theta) = v_{\min}$, which provides Eqs. (47) and (48), respectively.

The following proposition proves that $\hat{\theta}_b < \theta_b^*$, which is used by the subsequent lemma to prove that $v_b(\theta_b^*) = v_{\min}$.

Lemma 4 *For $d \in \mathbb{Z}^+$ and $v_{min} > 0$ we have $\hat{\theta}_b < u_{\hat{\theta}_b} < \ell_{\theta_b^*} \leq \theta_b^* < u_{\theta_b^*}$, where*

$$\ell_{\theta_b^*}(v_{min}) = \frac{1}{v_{min}^2} + \frac{\sqrt{v_{min}^2 + 16} - v_{min}}{4v_{min}^2} \tag{49}$$

$$u_{\theta_b^*}(v_{min}) = \frac{2}{v_{min}^2}. \tag{50}$$

Proof The proof can be found in Section 12.4.

Lemma 5 *For $v_{min} > 0$ and $d \in \mathbb{Z}^+$ we have $v_b(\theta) = v_{min}$ for $\theta \geq u_{\hat{\theta}_b}$, which includes $\theta \geq \theta_b^*$.*

Proof From Eq. (46) we have $u_{v_b^*}(\theta) = \frac{1}{\sqrt{\theta}}$, which is clearly monotonically decreasing with respect to θ. Therefore we have $u_{v_b^*}(\theta \geq u_{\hat{\theta}_b}) \leq v_{\min}$ and thus $v_b(\theta \geq u_{\hat{\theta}_b}) = v_{\min}$. In Lemma 4 it was proven that $\theta_b^* > u_{\hat{\theta}_b}$ and it thus follows that we have $v_b(\theta \geq \theta_b^*) = v_{\min}$, which completes the proof.

From Proposition 8 and Lemma 5 the maximum of $u_{r_b}(\theta, v_b; d, n_x)$ is at $\theta = \theta_b^*$ and $v_b = v_{\min}$, which is given by

$$\begin{aligned} u_{r_b}^*(v_{\min}, d, n_x) &= u_{r_b}(\theta_b^*(v_{\min}), v_{\min}) \\ &= 2(n_x - 1)\theta_b^* v_{\min} \left(1 + 2\sqrt{d}\,\theta_b^* v_{\min}\right) e^{-\theta_b^* v_{\min}^2} \\ &= 2(n_x - 1)\frac{4\sqrt{d} + \sqrt{v_{\min}^2 + 16d}}{v_{\min}^2} e^{-\frac{4\sqrt{d} + \sqrt{v_{\min}^2 + 16d} - v_{\min}}{4\sqrt{d}}}. \end{aligned} \tag{51}$$

7.4 Combined results for u_{r_a} and u_{r_b}

In Sections 8 and 9 the relative values of $\hat{\theta}_a$ and $\hat{\theta}_b$, and likewise θ_a^* and θ_b^*, are important and are considered in the following lemma and can be seen in Fig. 6a.

Lemma 6 *For $d \in \mathbb{Z}^+$ and $v_{min} > 0$ we have $\hat{\theta}_a(v_{min}, d) < \hat{\theta}_b(v_{min}, d)$ and $\theta_a^*(v_{min}, d) < \theta_b^*(v_{min}, d)$.*

Proof It is straightforward to prove that $\hat{\theta}_a(v_{\min}, d) < \hat{\theta}_b(v_{\min}, d)$ by comparing Eqs. (37) and (49) directly. Similarly, proving $\theta_a^*(v_{\min}, d) < \theta_b^*(v_{\min}, d)$ comes from showing that $\theta_a^*(v_{\min}, d) < \ell_{\theta_b^*}(v_{\min})$ using Eqs. (37) and (49).

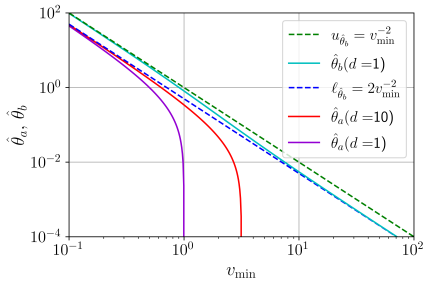

(a) Values of θ that satisfy $v_a^*(\hat{\theta}_a) = v_{\min}$ and $v_b^*(\hat{\theta}_b) = v_{\min}$, where $\hat{\theta}_a$ is calculated with Eq. (41), $\hat{\theta}_b$ is calculated with a root search, and its bounds coming from Eqs. (47) and (48).

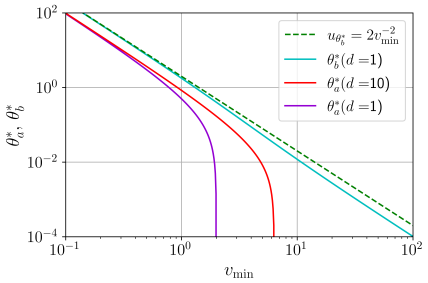

(b) Values θ_a^* and θ_b^* from Eqs. (37) and (43) that maximize $u_{r_a}(\theta)$ and $u_{r_b}(\theta)$, respectively, with Eqs. (49) and (50) providing the bounds for θ_b^*.

Fig. 6: Critical values of θ.

In this section v_a and v_b were bounded using $v_{\min}$ but not $v_{\max}$, i.e. the maximum Euclidean distance between points in the parameter space. It was proven in Proposition 6 that $v_a^*(\theta)$ is monotonically decreasing with respect to θ and it is clear from Eqs. (45) and (46) that $\ell_{v_b^*}(\theta)$ and $u_{v_b^*}(\theta)$ follow the same trend, which can also be seen in Fig. 7b. Therefore, using $v_{\max}$ to bound v_a and v_b would be most consequential for $\theta \to 0$, which is considered in the following lemma.

Lemma 7 *We have* $\lim_{\theta\to 0} u_{r_a} = n_x - 1$ *and* $\lim_{\theta\to 0} u_{r_b} = 0$.

Proof The proof can be found in Section 12.5.

The result of Lemma 7 can be seen in Fig. 4 for $n_x = 4$, $d = 10$, and $\theta = \frac{1}{2}$. The limit of both $u_{r_a}(\theta)$ and $u_{r_b}(\theta)$ for $\theta \to 0$, which is where v_a and v_b are largest, is small and finite. Therefore, $v_{\max}$ does not play an important role in bounding r_a and r_b, which is why it is omitted from $v_a(\theta; v_{\min}, d)$ and $v_b(\theta; v_{\min}, d)$.

The use of Eqs. (35) and (36) to bound the eigenvalues of K_∇ can be seen in Fig. 8a for $d = 2$, $n_x = 10$, and $v_{\min} = 2\sqrt{2}$. Meanwhile, Fig. 8b compares the condition number and its bound from Eq. (23) and $\eta_{\mathsf{K}_\nabla} = 10^{-8}$. The rapid reduction in the bound for the condition number in Fig. 8b coincides with the value of θ when $\ell_{\lambda_{\min}} = 0$, as can be seen in Fig. 8a for the case with $v_{\min} = 2\sqrt{d}$.

Unlike for the gradient-free case, the condition number of K_∇ is not monotonically decreasing with respect to θ, as shown in Fig. 8b. The reason for this is explored by exploring the structure of K_∇ as θ gets progressively larger. As was proven in Propositions 4 and 8, there is a unique maximum for $u_{r_a}(\theta, v_a(\theta))$ and $u_{r_b}(\theta, v_b(\theta))$, respectively. It is also straightforward to verify that both of these bounds go to zero as $\theta \to \infty$, and this can be seen in Fig. 5 for the case with $n_x = 4$, $d = 10$ and $v_{\min} = \sqrt{2}$. As a result, for

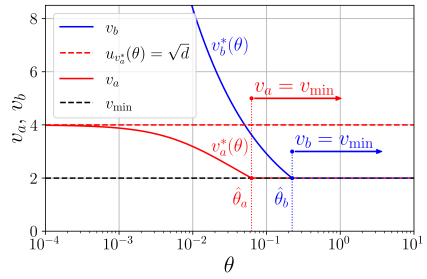

(a) The functions $v_a(\theta)$ and $v_b(\theta)$ are from Eqs. (30) and (33), respectively, and $u_{v_a^*}$ comes from Eq. (40), with $d = 16$ and $v_{\min} = 2$.

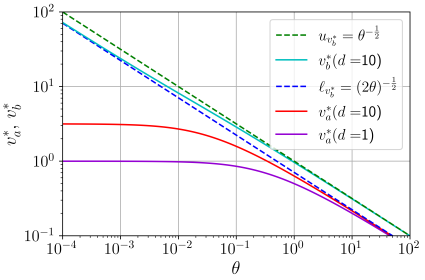

(b) Functions $v_a^*(\theta; d)$ and $v_b^*(\theta; d)$ from Eqs. (38) and (44), respectively, while the bounds on $v_b^*(\theta; d)$ come from Eqs. (45) and (46).

Fig. 7: The role of $v_a(\theta)$ and $v_b(\theta)$ for the upper bounds $u_{r_a}(\theta, v_a(\theta))$ and $u_{r_b}(\theta, v_b(\theta))$, respectively.

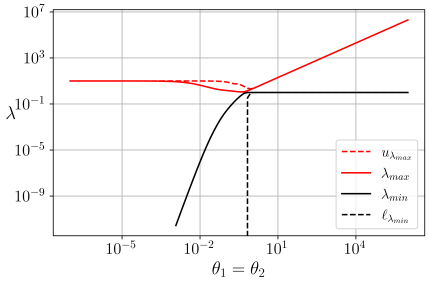

(a) Values and bounds of $\lambda_{\min}$ and $\lambda_{\max}$ for K with $v_{\min} = 2\sqrt{d}$ from Eqs. (35) and (36), respectively.

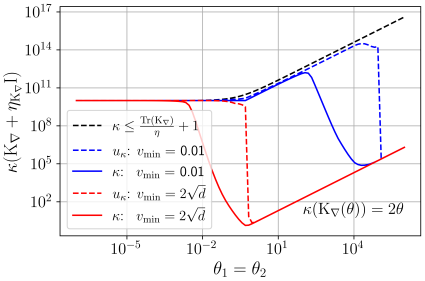

(b) Plots of $\kappa\left(\mathsf{K}_\nabla(\theta) + \eta_{\mathsf{K}_\nabla}\mathsf{I}\right)$ with $\eta_{\mathsf{K}_\nabla} = 10^{-8}$ along with its bounds from Eq. (23).

Fig. 8: Case with $d = 2$ and $n_x = 10$.

$\theta > \theta_b^* > \theta_a^*$, the sum of the absolute value of the off-diagonal entries of K_∇ become progressively smaller and the last $n_x \cdot d$ diagonal entries get larger as θ increases. From Eq. (21) it follows that once $\ell_{\lambda_{\min}} > 0$, K_∇ is strictly diagonally dominant and its condition number can be approximated with

$$\kappa(\mathsf{K}_\nabla(\theta)) \approx \kappa(\mathrm{diag}(\mathsf{K}_\nabla(\theta))) = \begin{cases} \frac{1}{2\theta} & \text{if } \theta < \frac{1}{2} \\ 2\theta & \text{if } \theta \geq \frac{1}{2}. \end{cases} \tag{52}$$

Fig. 8b shows that Eq. (52) provides a good approximation of the condition number of K_∇ when θ is sufficiently large. In order to see the same trend for $\theta < \frac{1}{2}$, $v_{\min}$ would need to be even larger. Also, it is clear from Eqs. (29) and (32) that K_∇ is a diagonal matrix when $n_x = 1$. The consequence of Eq. (52) is that, unlike for the gradient-free case, it is not possible to bound the condition number of K_∇ for all $\theta > 0$. The following remark explains why this is not a practical limitation.

Remark 1 The condition number of $\mathsf{K}_\nabla(\theta)$ is unbounded as $\theta \to \infty$. However, it is only important to have $\kappa\left(\mathsf{K}_\nabla(\theta) + \eta_{\mathsf{K}_\nabla}\mathsf{I}\right) \leq \kappa_{\max}$ for values of θ that are likely to maximize Eq. (12). When $\ell_{\lambda_{\min}}(\theta) \geq 0$, K_∇ is diagonally dominant, which implies that the off-diagonal entries, i.e. the cross-correlations, are small relative to the diagonal entries. Therefore, values of θ that provide a diagonally dominant K_∇ result in a surrogate where the data is weakly correlated and thus unlikely to maximize the marginal log-likelihood from Eq. (12). As such, we are only interested in ensuring $\kappa\left(\mathsf{K}_\nabla(\theta) + \eta_{\mathsf{K}_\nabla}\mathsf{I}\right) \leq \kappa_{\max}$ while $\ell_{\lambda_{\min}}(\theta) \leq 0$.

8 Bounding $\kappa(\mathsf{K}_\nabla(\boldsymbol{\theta}) + \eta_{\mathsf{K}_\nabla}\mathsf{I})$ with the minimum η_{K_∇}

8.1 Optimization problem

To ensure we have $\kappa\left(\mathsf{K}_\nabla + \eta_{\mathsf{K}_\nabla}\mathsf{I}\right) \leq \kappa_{\max}$ we use both η_{K_∇} and $v_{\min}$. In this section we are interested in identifying the smallest value of η_{K_∇} first and then using this to identify the required $v_{\min}$ such that the condition number of $\mathsf{K}_\nabla + \eta_{\mathsf{K}_\nabla}\mathsf{I}$ remains below the user-set thresholds of $\kappa_{\max}$. We thus have the following successive optimization problems

$$\eta_{\mathsf{K}_\nabla} = \underset{\eta}{\operatorname{argmin}}\, \eta \quad \text{such that } \lim_{\theta\to 0} \kappa\left(\mathsf{K}_\nabla(\theta) + \eta\mathsf{I}\right) \leq \kappa_{\max} \tag{53}$$

$$v_{\min} = \underset{v}{\operatorname{argmin}}\, v \quad \text{such that } \kappa\left(\mathsf{K}_\nabla(\theta; v) + \eta_{\mathsf{K}_\nabla}\mathsf{I}\right) \leq \kappa_{\max} \text{ while } \ell_{\lambda_{\min}}(\theta; v) \leq 0, \tag{54}$$

where the solution to Eq. (53) is used to solve Eq. (54) along with $\theta > 0$. The constraint in Eq. (54) is only active while $\ell_{\lambda_{\min}}(\theta; v) \leq 0$, as explained in Remark 1. In Section 8.2 it is proven that the solution to Eq. (53) is $\eta_{\mathsf{K}_\nabla} = \eta_{\mathsf{K}} = \frac{n_x}{\kappa_{\max}-1}$. Next, it is proven in Section 8.3 that the solution to Eq. (54) is $v_{\min} = 2\sqrt{d}$. Finally, the following remark provides additional information on the solutions of Eqs. (53) and (54).

Remark 2 Values for η_{K_∇} and $v_{\min}$ to ensure $\kappa(\mathsf{K}_\nabla(\theta; v_{\min}) + \eta_{\mathsf{K}_\nabla}\mathsf{I}) \leq \kappa_{\max}$ are found by using the upper bounds derived in Section 7.1 for $r_a(\theta)$ and $r_b(\theta)$. The functions $u_{r_a}(\theta, v_a(\theta))$ and $u_{r_b}(\theta, v_b(\theta))$ are not strict upper bounds on $r_a(\theta)$ and $r_b(\theta)$. As such, it is possible to ensure $\kappa(\mathsf{K}_\nabla(\theta; v_{\min}) + \eta_{\mathsf{K}_\nabla}\mathsf{I}) \leq \kappa_{\max}$ with values of η_{K_∇} and $v_{\min}$ smaller than what is derived using $u_{r_a}(\theta, v_a(\theta))$ and $u_{r_b}(\theta, v_b(\theta))$.

8.2 Solution to Eq. (53)

The following proposition provides the solution to Eq. (53).

Proposition 10 *The solution to Eq. (53) for $n_x \in \mathbb{Z}^+$ is $\eta_{\mathsf{K}_\nabla} = \frac{n_x}{\kappa_{\max}-1}$.*

Proof From Lemma 7 we have $\lim_{\theta\to 0} u_{r_a}(\theta) = n_x - 1$ and $\lim_{\theta\to 0} u_{r_b}(\theta) = 0$, and we thus have from Eqs. (35) and (36)

$$\lim_{\theta\to 0} u_{\lambda_{\max}}(\theta) = \lim_{\theta\to 0} \max\left(1 + u_{r_a}(\theta), 2\theta + u_{r_b}(\theta)\right) = n_x \tag{55}$$

$$\lim_{\theta\to 0} \ell_{\lambda_{\max}}(\theta) = \lim_{\theta\to 0} \min\left(1 - u_{r_a}(\theta), 2\theta - u_{r_b}(\theta)\right) = \min(2 - n_x, 0). \tag{56}$$

We assume $\lambda_{\max} = u_{\lambda_{\max}} = n_x$ and $\lambda_{\min} = \max(0, \ell_{\lambda_{\min}}) = 0$ to consider the worst-case scenario for bounding $\kappa\left(\mathsf{K}_\nabla + \eta_{\mathsf{K}_\nabla}\mathsf{I}\right)$. Using these values of $\lambda_{\min}$ and $\lambda_{\max}$ along with Lemma 1, which assumes $\lambda_{\min} = 0$, we find that we can ensure $\kappa(\mathsf{K}_\nabla(\theta \to 0) + \eta_{\mathsf{K}_\nabla}\mathsf{I}) \leq \kappa_{\max}$ with $\eta_{\mathsf{K}_\nabla} = \frac{n_x}{\kappa_{\max}-1}$, which completes the proof.

Proposition 10 indicates that it is possible to have $\kappa(\mathsf{K}_\nabla + \eta_{\mathsf{K}_\nabla}\mathsf{I}) \leq \kappa_{\max}$ and $\kappa(\mathsf{K} + \eta_{\mathsf{K}}\mathsf{I}) \leq \kappa_{\max}$ with $\eta_{\mathsf{K}_\nabla} = \eta_{\mathsf{K}} = \frac{n_x}{\kappa_{\max}-1}$, where η_{K} comes from Eq. (16). The same nugget value can thus ensure that K and K_∇ have a condition number below the same user-set threshold even though the latter matrix has $d+1$ times as many rows and columns as the former. The following subsection provides the solution to Eq. (54).

8.3 Solution to Eq. (54)

The following lemma proves that $v_{\min} \geq 2\sqrt{d}$ is necessary in order to satisfy the constraint in Eq. (54).

Lemma 8 *Having $v_{min} \geq 2\sqrt{d}$ when $\eta_{\mathsf{K}_\nabla} = \eta_{\mathsf{K}} = \frac{n_x}{\kappa_{\max}-1}$ is a necessary condition to have $\kappa\left(\mathsf{K}_\nabla(\theta) + \eta_{\mathsf{K}_\nabla}\mathsf{I}\right) \leq \kappa_{\max}$ while $\ell_{\lambda_{min}} \leq 0$.*

Proof From Proposition 10 the solution to Eq. (53) is $\eta_{\mathsf{K}_\nabla} = \eta_{\mathsf{K}} = \frac{n_x}{\kappa_{\max}-1}$. To ensure we have $\kappa(\mathsf{K}_\nabla(\theta) + \eta_{\mathsf{K}_\nabla}\mathsf{I}) \leq \kappa_{\max}$ we require that $u_{\lambda_{\max}}(\theta) \leq n_x$ while $\ell_{\lambda_{\min}} \leq 0$. From Lemma 7 we have $1 + u_{r_a}(\theta \to 0) = n_x$. Therefore, to have $u_{\lambda_{\max}}(\theta) \leq n_x$, which depends on $1 + u_{r_a}(\theta)$ from Eq. (36), $u_{r_a}(\theta)$ must be monotonically decreasing for $\theta > 0$. From Propositions 4 and 7, the maximum of $u_{r_a}(\theta)$ is at

$$\theta_a^*(v_{\min}, d) = \max\left(0, \frac{2\sqrt{d} - v_{\min}}{2\sqrt{d}v_{\min}^2}\right).$$

To ensure $u_{r_a}(\theta)$ is monotonically decreasing for $\theta > 0$, we need $\theta_a^* \leq 0$ and thus $v_{\min} \geq 2\sqrt{d}$, which completes the proof.

Corollary 1 *From Lemma 8 and Eq. (36) it follows that when $v_{min} \geq 2\sqrt{d}$, we can only have $u_{\lambda_{max}} > n_x$ if $2\theta + u_{r_b}(\theta) > n_x$ since $1 + u_{r_a}(\theta) \leq n_x \; \forall\theta > 0$.*

We now calculate $u_{r_a}(\theta, v_a)$, $u_{r_b}(\theta, v_b)$, as well as $\theta_b^*(v_{\min})$ with $v_a = v_b = v_{\min} = 2\sqrt{d}$

$$\theta_b^*\left(v_{\min} = 2\sqrt{d}\right) = \frac{1+\sqrt{5}}{8d} \tag{57}$$

$$\begin{aligned} u_{r_a}\left(\theta, v_a = 2\sqrt{d}\right) &= (n_x - 1)\left(1 + 4d\theta\right) e^{-4d\theta} \\ &= (n_x - 1) g_a(\theta; d) \end{aligned} \tag{58}$$

$$\begin{aligned} u_{r_b}\left(\theta, v_b = 2\sqrt{d}\right) &= (n_x - 1) 4\sqrt{d}\,\theta g_a(\theta; d) \\ &= (n_x - 1) g_b(\theta; d), \end{aligned} \tag{59}$$

where $g_a(\theta; d) = (1 + 4d\theta)\, e^{-4d\theta}$ and $g_b(\theta; d) = 4\sqrt{d}\,\theta g_a(\theta; d)$. From Corollary 1 the maximum of $u_{\lambda_{\max}}$ depends on $2\theta + u_{r_b}(\theta)$, which depends on $g_b(\theta; d)$ from Eq. (59). The next lemma considers the maximum of $g_b(\theta; d)$.

Lemma 9 *For $d \in \mathbb{Z}^+$ and $\theta > 0$ we have $g_b(\theta; d) \leq g_b^*(d) < 1$, where*

$$g_b^*(d) = \left(\frac{2+\sqrt{5}}{\sqrt{d}}\right) e^{-\frac{1+\sqrt{5}}{2}}. \tag{60}$$

Proof It is straightforward to derive Eq. (60) with $g_b(\theta; d)$ from Eq. (59) and $\theta = \theta_b^*$ from Eq. (57). The maximum of $g_b^*(d)$ for $d \in \mathbb{Z}^+$ is at $d = 1$ since it is monotonically decreasing with respect to d. We thus have

$$g_b(\theta; d) \leq g_b^*(d) \leq g_b^*(1) = \left(\frac{2+\sqrt{5}}{\sqrt{1}}\right) e^{-\frac{1+\sqrt{5}}{2}} \approx 0.84,$$

which completes the proof.

The next proposition considers the maximum of $u_{\lambda_{\max}}(\theta)$ for the range $0 < \theta \leq \frac{1}{2}$.

Lemma 10 *For $0 < \theta \leq \frac{1}{2}$ we have $u_{\lambda_{max}}(\theta) \leq n_x$ when $v_{min} = 2\sqrt{d}$, $d \in \mathbb{Z}^+$, and $n_x \in \mathbb{Z}^+ \setminus 1$.*

Proof From Corollary 1 it follows that we can only have $u_{\lambda_{\max}}(\theta) > n_x$ when $2\theta + u_{r_b}(\theta) > n_x$ when $v_{\min} = 2\sqrt{d}$. Therefore, we consider the maximum of $2\theta + u_{r_b}(\theta)$ for $0 < \theta \leq \frac{1}{2}$. From Eqs. (59) and (60) we have

$$\begin{aligned} \max_{0<\theta\leq\frac{1}{2}} \left(2\theta + u_{r_b}(\theta; v_b(\theta))\right) &< \max_{0<\theta\leq\frac{1}{2}} 2\theta + \max_{0<\theta\leq\frac{1}{2}} u_{r_b}(\theta; v_b(\theta)) \\ &= 2\frac{1}{2} + (n_x - 1) g_b^* \\ &< n_x, \end{aligned}$$

where $g_b^* < 1$ comes from Lemma 9, which completes the proof.

It is impossible to ensure $u_{\lambda_{\max}}(\theta) < n_x \, \forall \, \theta > 0$ since the function $2\theta + u_{r_b}(\theta)$ is unbounded with respect to θ. The two following proposition prove that when $u_{\lambda_{\max}}(\theta) > n_x$, we also have $\ell_{\lambda_{\min}}(\theta) > 0$.

Proposition 11 *For $v_{min} = 2\sqrt{d}$, $d \in \mathbb{Z}^+$, and $n_x \in \mathbb{Z}^+ \setminus 1$, we have $(1 - u_{r_a}(\theta)) > 0$ when $u_{\lambda_{max}}(\theta) > n_x$.*

Proof The proof can be found in Section 13.1.

Proposition 12 *For $v_{min} = 2\sqrt{d}$, $d \in \mathbb{Z}^+$, and $n_x \in \mathbb{Z}^+ \setminus 1$, we have $(2\theta - u_{r_b}(\theta)) > 0$ when $u_{\lambda_{max}}(\theta) > n_x$.*

Proof The proof is in Section 13.2.

As a result of Propositions 11 and 12 we have $\ell_{\lambda_{\min}}(\theta) > 0$ when $u_{\lambda_{\max}}(\theta) > n_x$, $d \in \mathbb{Z}^+$, $n_x \in \mathbb{Z}^+ \setminus 1$, and $v_{\min} = 2\sqrt{d}$. From Lemma 8 it follows that $v_{\min} = 2\sqrt{d}$ is also the minimum required value for $v_{\min}$, which means it is the solution to Eq. (54).

9 Bounding $\kappa(\mathsf{K}_\nabla(\theta) + \eta_{\mathsf{K}_\nabla}\mathsf{I})$ with the minimum $v_{\min}$

9.1 Optimization problem

In the previous section we set $\eta_{\mathsf{K}_\nabla} = \eta_{\mathsf{K}}$ and then found the minimum $v_{\min}$ to ensure $\kappa\left(\mathsf{K}_\nabla + \eta_{\mathsf{K}_\nabla}\mathsf{I}\right) \leq \kappa_{\max}$. In this section we reverse the order and solve first for $v_{\min}$ and then for η_{K_∇} with the following optimization problems

$$v_{\min} = \underset{v}{\operatorname{argmin}}\, v \quad \text{such that } \ell_{\lambda_{\min}}(\theta; v) > 0, \forall\, \theta > \frac{1}{2} \tag{61}$$

$$\eta_{\mathsf{K}_\nabla} = \underset{\eta}{\operatorname{argmin}}\, \eta \quad \text{such that } \kappa\left(\mathsf{K}_\nabla(\theta; v_{\min}) + \eta\mathsf{I}\right) \leq \kappa_{\max} \, \forall\, \theta \in \left(0, \frac{1}{2}\right]. \tag{62}$$

Just like in Section 8, Remark 2 applies to the optimization of Eqs. (61) and (62) and the constraint in Eq. (62) is only active while $\ell_{\lambda_{\min}}(\theta; v) \leq 0$, as explained in Remark 1. The cut-off $\theta = \frac{1}{2}$ was selected since it is at this value that all the diagonal entries in K_∇ are equal. The solution for Eq. (61) is derived in Section 9.2 and Section 9.3 provides the solution to Eq. (62).

9.2 Solution to Eq. (61)

Sufficient but not necessary conditions to ensure that the constraint in Eq. (61) is satisfied involve having $\ell_{\lambda_{\min}}(\theta) \geq 0$ at $\theta = \frac{1}{2}$ and $\ell_{\lambda_{\min}}(\theta)$ be monotonically increasing for $\theta \geq \frac{1}{2}$. The two following lemmas consider these requirements.

Lemma 11 *For $d \in \mathbb{Z}^+$, $n_x \in \mathbb{Z}^+ \setminus 1$, and $v_{min} \geq \sqrt{2}$, a necessary and sufficient condition to have $\ell_{\lambda_{min}} = 0$ at $\theta = \frac{1}{2}$ is $2\theta - u_{r_b}(\theta, v_b(\theta; v_{min})) = 0$.*

Proof We have from Lemma 6 and Eq. (47) $\hat{\theta}_a < \hat{\theta}_b < u_{\hat{\theta}_b} = \frac{1}{v_{\min}^2} \leq \frac{1}{2}$ when $v_{\min} \geq \sqrt{2}$. From Proposition 7 and Lemma 5 we thus have $v_a(\theta) = v_b(\theta) = v_{\min}$ for $\theta \geq \frac{1}{2}$. We now compare $2\theta - u_{r_b}(\theta, v_{\min})$ and $1 - u_{r_a}(\theta, v_{\min})$ at $\theta = \frac{1}{2}$

$$\begin{aligned}
[2\theta - u_{r_b}(\theta)]_{\theta=\frac{1}{2}} &= 1 - v_{\min}(n_x - 1)\left(1 + \sqrt{d}v_{\min}\right) e^{-\frac{v_{\min}^2}{2}} \\
&= 1 - v_{\min} u_{r_a}\left(\theta = \frac{1}{2}\right) \\
&< 1 - u_{r_a}\left(\theta = \frac{1}{2}\right),
\end{aligned}$$

where the last inequality holds since $v_{\min} \geq \sqrt{2}$ and $u_{r_a} > 0$. From Eq. (35) it follows that having $\ell_{\lambda_{\min}} > 0$ at $\theta = \frac{1}{2}$ requires $1 - u_{r_a}(\theta, v_a(\theta)) \geq 0$ and $2\theta - u_{r_b}(\theta, v_b(\theta)) \geq 0$. Since we have shown that $2\theta - u_{r_b} < 1 - u_{r_a}$, it follows that having $2\theta - u_{r_b}(\theta, v_{\min}) = 0$ at $\theta = \frac{1}{2}$ is necessary and sufficient to have $\ell_{\lambda_{\min}} = 0$, which completes the proof.

Lemma 12 *For $\theta \geq \frac{1}{2}$, $d \in \mathbb{Z}^+$, and $n_x \in \mathbb{Z}^+ \setminus 1$, having $v_{min} \geq 2$ is a sufficient condition to ensure $\ell_{\lambda_{min}}(\theta)$ is monotonically increasing.*

Proof With $v_{\min} \geq 2$ we have from Lemma 6 and Eq. (50) $\theta_a^* < \theta_b^* < u_{\theta_b^*} = \frac{2}{v_{\min}^2} \leq \frac{1}{2}$. Therefore, for $\theta \geq \frac{1}{2}$, both $1 - u_{r_a}^*(\theta)$ and $2\theta - u_{r_b}^*(\theta)$ are monotonically increasing, which also applies to $\ell_{\lambda_{\min}}(\theta)$ and this completes the proof.

The following proposition combines the results from the last two lemmas to derive the solution to Eq. (61).

Proposition 13 *For $d \in \mathbb{Z}^+$ and $n_x \in \mathbb{Z}^+ \setminus 1$ the constraint in Eq. (61) is satisfied with $v_{min} \geq v_{req}$ and the solution to Eq. (61) is $v_{min} = v_{req}$, where v_{req} is the solution to the following transcendental equation*

$$(n_x - 1)v_{req}\left(1 + \sqrt{d}v_{req}\right) e^{-\frac{v_{req}^2}{2}} = 1 \quad \textit{where } v_{req} > \sqrt{2}. \tag{63}$$

Proof The proof can be found in Section 14.1.

Eq. (63) requires a root search to solve for v_{req}. The next proposition presents a simple algebraic equation that provides $\tilde{v}_{\text{req}} > v_{\text{req}}$.

Proposition 14 *Having $v_{min} \geq \tilde{v}_{req} > v_{req}$ ensures the constraint in Eq. (61) is satisfied for $d \in \mathbb{Z}^+$, and $n_x \in \mathbb{Z}^+ \setminus 1$, where*

$$\tilde{v}_{req}(d, n_x) = \frac{2 + \sqrt{4 + 2e^2 \ln\left(\frac{(n_x - 1)\left(1 + 2\sqrt{d}\right)}{2}\right)}}{e}. \tag{64}$$

Proof The proof can be found in Section 14.2.

9.3 Selecting η_{K_∇} to ensure $\kappa\left(\mathsf{K}_\nabla + \eta_{\mathsf{K}_\nabla}\mathsf{I}\right) \leq \kappa_{\max}$ for $0 < \theta \leq \frac{1}{2}$

In this subsection we derive the solution to Eq. (62). To ensure $\kappa(\mathsf{K}_\nabla(\theta) + \eta_{\mathsf{K}_\nabla}\mathsf{I}) \leq \kappa_{\max}$ for $0 < \theta \leq \frac{1}{2}$, the parameter η_{K_∇} must be selected by considering the maximum of $u_{\lambda_{\max}}$ for $0 < \theta \leq \frac{1}{2}$, which is considered in the next proposition. The case for $v_{\min} > 2\sqrt{d}$ is not considered since it was shown in Section 8 that using $v_{\min} = 2\sqrt{d}$ provides the minimum requires η_{K_∇} to ensure $\kappa\left(\mathsf{K}_\nabla + \eta_{\mathsf{K}_\nabla}\mathsf{I}\right) \leq \kappa_{\max}$. Therefore, there is no benefit to having $v_{\min} > 2\sqrt{d}$.

Proposition 15 *We have $u_{\lambda_{max}} = 1 + u^*_{r_a}$ for $0 < \theta \leq \frac{1}{2}$, $d \in \mathbb{Z}^+$, $n_x \in \mathbb{Z}^+ \setminus 1$, and $v_{req} \leq v_{min} \leq 2\sqrt{d}$, where $u^*_{r_a}$ and v_{req} come from Eqs. (65) and (63), respectively.*

Proof The proof can be found in Section 14.3.

The following proposition provides the solution to Eq. (62).

Proposition 16 *For $v_{req} \leq v_{min} \leq 2\sqrt{d}$, $d \in \mathbb{Z}^+$, and $n_x \in \mathbb{Z}^+ \setminus 1$, we can ensure $\kappa\left(\mathsf{K}_\nabla + \eta_{\mathsf{K}_\nabla}\mathsf{I}\right) \leq \kappa_{\max}$ for $0 < \theta \leq \frac{1}{2}$ with*

$$\eta_{\mathsf{K}_\nabla}(v_{min}, d, n_x) = \frac{1 + (n_x - 1)\frac{2\sqrt{d}}{v_{min}} e^{\frac{v_{min}}{2\sqrt{d}} - 1}}{\kappa_{\max} - 1}. \tag{65}$$

Proof From Proposition 15 and Eq. (15), we can ensure $\kappa\left(\mathsf{K}_\nabla + \eta_{\mathsf{K}_\nabla}\mathsf{I}\right) \leq \kappa_{\max}$ for $0 < \theta \leq \frac{1}{2}$, $d \in \mathbb{Z}^+$, and $n_x \in \mathbb{Z}^+ \setminus 1$ with $v_{\min} \geq v_{\text{req}}$ and

$$\begin{aligned}
\eta_{\mathsf{K}_\nabla} &\geq \frac{\max_{0<\theta\leq\frac{1}{2}} u_{\lambda_{\max}}(\theta; v_{\min})}{\kappa_{\max} - 1} \\
&= \frac{1 + u^*_{r_a}}{\kappa_{\max} - 1} \\
&= \frac{1 + (n_x - 1)\frac{2\sqrt{d}}{v_{\min}} e^{\frac{v_{\min}}{2\sqrt{d}} - 1}}{\kappa_{\max} - 1},
\end{aligned}$$

where Eq. (42) was used for $u^*_{r_a}$ and this matches Eq. (65), which completes the proof.

From Eq. (65) we recover $\eta_{\mathsf{K}_\nabla} = \eta_{\mathsf{K}} = \frac{n_x}{\kappa_{\max} - 1}$ when $v_{\min} = 2\sqrt{d}$, which is consistent with the results from Section 8.

10 Results and discussion

10.1 Required $v_{\min}$ and η_{K_∇}

The results from Sections 8 and 9 are combined to provide a required value of $v_{\min}$ that is smaller than either individual section while ensuring

$\kappa(\mathsf{K}_\nabla(\boldsymbol{\theta}) + \eta_{\mathsf{K}_\nabla}\mathsf{I}) \leq \kappa_{\max}$ when $\boldsymbol{\theta} = \theta\mathbf{1}$. Either of the following equations can be used

$$v_{\min,\text{set}}(d, n_x; \rho) = \frac{\min\left(2\sqrt{d}, v_{\text{req}}(d, n_x)\right)}{\rho} \tag{66}$$

$$v_{\min,\text{set}}(d, n_x; \rho) = \frac{\min\left(2\sqrt{d}, \tilde{v}_{\text{req}}(d, n_x)\right)}{\rho}, \tag{67}$$

where $\rho \geq 1$ is a user-set parameter, while v_{req} and $\tilde{v}_{\text{req}}$ are given by Eqs. (63) and (64), respectively. Having $0 < \rho \leq 1$ ensures $\kappa(\mathsf{K}_\nabla(\boldsymbol{\theta}) + \eta_{\mathsf{K}_\nabla}\mathsf{I}) \leq \kappa_{\max}$ when $\boldsymbol{\theta} = \theta\mathbf{1}$. While $\rho > 1$ does not ensure $\kappa(\mathsf{K}_\nabla(\boldsymbol{\theta}) + \eta_{\mathsf{K}_\nabla}\mathsf{I}) \leq \kappa_{\max}$, using a modest value for ρ, such as $\rho = 10$, is still sufficient in practice to ensure $\kappa(\mathsf{K}_\nabla(\boldsymbol{\theta}) + \eta_{\mathsf{K}_\nabla}\mathsf{I}) \leq \kappa_{\max}$ since the bounds u_{r_a} and u_{r_b} are not tight. This is demonstrated in Section 10.3. The benefit to having $\rho > 1$ is to accelerate the optimization, as shown in Section 10.6.

Eq. (66) provides a smaller value for $v_{\min,\text{set}}$ than using Eq. (67), but it requires solving Eq. (63) with a root search for v_{req}. However, as is shown in Fig. 9a, Eq. (67) provides a solution that is nearly identical to the one from Eq. (66) and no root search is required to solve for $\tilde{v}_{\text{req}}$.

Fig. 9b plots the fraction of η_{K_∇} to η_{K}, which are calculated with Eqs. (65) and (16), respectively. The nugget $\eta_{\mathsf{K}_\nabla}(v_{\min,\text{set}}, d, n_x)$ is calculated with $v_{\min,\text{set}}(d, n_x)$ from both Eqs. (66) and (67). An additional benefit to using Eq. (67) instead of Eq. (66) is that the former requires a slightly smaller η_{K_∇} than the latter. For a given n_x, the matrix K_∇ has $d+1$ times as many rows and columns as K. Nonetheless, Fig. 9b demonstrates that when Eqs. (66) or (67) is used to set $v_{\min}$ for X, K_∇ only requires a nugget that is marginally larger than what is required for K to ensure the condition number of these matrices is smaller than $\kappa_{\max}$. For example, with $d \in \{5, 25, 100\}$ in the worst-case scenario for n_x we only require η_{K_∇} to be approximately 1.1, 1.5, and 2.2 times as large as η_{K}, respectively.

10.2 Consequence of increasing $v_{\min}$

In Sections 8 and 9 it was proven that having $v_{\min} \geq v_{\min,\text{set}}$ ensures $\kappa(\mathsf{K}_\nabla(\boldsymbol{\theta}) + \eta_{\mathsf{K}_\nabla}\mathsf{I}) \leq \kappa_{\max}$ when $\boldsymbol{\theta} = \theta\mathbf{1}$. In this section it is demonstrated that there is a consequence to increasing $v_{\min}$, namely that this increases the difference between the gradient of the surrogate and of the function of interest at evaluation points. To demonstrate this, a Latin hypercube sampling was used to create a set of $n_x = 10$ points where the Rosenbrock function from Eq. (20) was evaluated. The matrix X was rescaled isotropically and Eq. (12) was solved with a gradient-based optimizer and five different initial solutions $\boldsymbol{\theta} \in [10^{-8}, 10^{8}]^2$. The parameters $\kappa_{\max} = 10^{15}$ and $\eta_{\mathsf{K}_\nabla} = 10^{-7}$ were selected so that the constraint on the condition number was not active. Fig. 10a shows the relation between rescaling X isotropically and the solution $\bar{\boldsymbol{\theta}}$ to Eq. (12) when the constraint on the condition number is not active. The slope of the lines

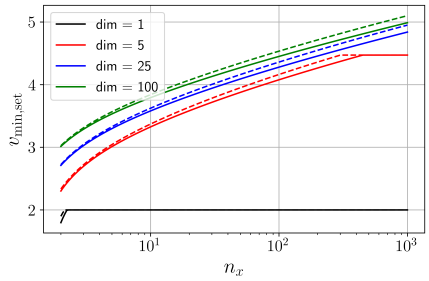

(a) Solution to Eqs. (66) and (67) with $\rho = 1$.

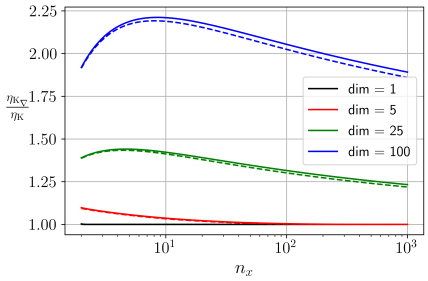

(b) Solution to Eq. (65) with $v_{\min} = v_{\min,\text{set}}$ from Eqs. (66) and (67) with $\rho = 1$.

Fig. 9: Ensuring $\kappa\left(\mathsf{K}_\nabla(\theta) + \eta_{\mathsf{K}_\nabla}\mathsf{I}\right) \leq \kappa_{\max}$ with $v_{\min} \geq v_{\min,\text{set}}$ and the minimum η_{K_∇}. Solid lines are for Eq. (66), while dashed lines are for Eq. (67).

using a least squares fit are -1.9 and -1.8 for θ_1 and θ_2, respectively. The inverse quadratic relationship between the scaling of X and $\boldsymbol{\theta}$ from Eq. (1) indicates that the theoretical slope should be -2 on a log-log plot. The small difference between the theoretical and observed slopes is thought to be primarily due to the non-zero nugget.

In Fig. 10b we can see that as $v_{\min}$ increases, so does the difference between the gradient of the surrogate and of the function of interest where Eq. (20) was evaluated. However, if η_{K_∇} was zero instead of 10^{-7}, then the difference between the gradient of the surrogate and of the function of interest would be on the order of machine precision, as long as the condition number of K_∇ is not too large. The last $n_x \cdot d$ diagonal entries in $\mathsf{K}_\nabla + \eta_{\mathsf{K}_\nabla}$ are $2\theta + \eta_{\mathsf{K}_\nabla}$. Therefore, as θ gets smaller, which is a consequence of $v_{\min}$ getting larger as seen in Fig. 10a, then η_{K_∇} makes a larger relative change to the diagonal entries of the matrix K_∇. This leads to the increased difference between the gradient of the surrogate and of the function of interest shown in Fig. 10b. There is thus a trade-off between increasing $v_{\min}$ sufficiently to ensure the condition number of the covariance matrix is below a user-set threshold, but not too much since it increases the difference between the gradient of the surrogate and of the function of interest.

10.3 Impact of rescaling X on $\kappa(\mathsf{K}_\nabla(\boldsymbol{\theta}) + \eta_{\mathsf{K}_\nabla}\mathsf{I})$

A Latin hypercube sampling with the domain $[-1, 1]^2$ was used to create data sets with $n_x = 10$ and $n_x = 50$. The matrix X was rescaled isotropically using Eq. (27) to have three different minimum Euclidean distances between data points. For all cases $\eta_{\mathsf{K}_\nabla}(n_x) = \eta_{\mathsf{K}}(n_x)$ from Eq. (16) was used. With $v_{\min} = 0.01$ we can see from Figs. 11a and 11d that there are large regions of the hyperparameter space where $\kappa(\mathsf{K}_\nabla(\boldsymbol{\theta}) + \eta_{\mathsf{K}_\nabla}\mathsf{I}) > \kappa_{\max}$, including where the marginal likelihood from Eq. (12) is maximized. We can ensure $\kappa(\mathsf{K}_\nabla(\boldsymbol{\theta}) + \eta_{\mathsf{K}_\nabla}\mathsf{I}) \leq \kappa_{\max}$ when $\boldsymbol{\theta} = \theta\mathbf{1}$ and $v_{\min}$ is calculated using Eq. (67)

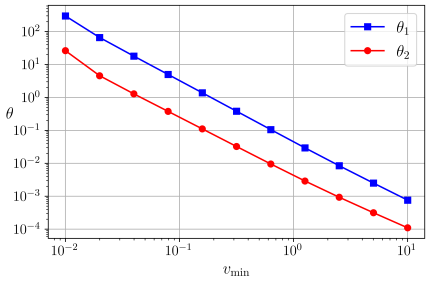

(a) Impact of rescaling X isotropically on the solution $\bar{\boldsymbol{\theta}}$ to Eq. (12).

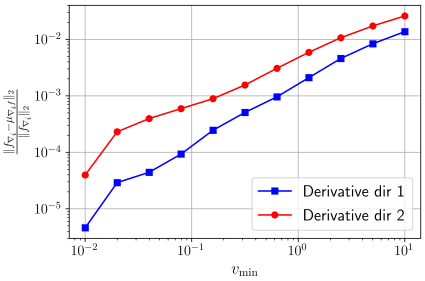

(b) Difference between the gradient of the surrogate and of the function of interest at evaluation points as a function of $v_{\min}$.

Fig. 10: The consequence of rescaling X isotropically in order to increase $v_{\min}$.

with $\rho = 1$. This is shown in Figs. 11c and 11f where $\kappa(\mathsf{K}_\nabla(\boldsymbol{\theta}) + \eta_{\mathsf{K}_\nabla}\mathsf{I}) \leq \kappa_{\max}$ when $\boldsymbol{\theta} = \theta\mathbf{1}$ and also for most of $\boldsymbol{\theta} \in [10^{-8}, 10^{8}]^2$. Finally, Figs. 11b and 11e consider the case when $v_{\min}$ is calculated using Eq. (67) with $\rho = 10$. While this case does not ensure $\kappa(\mathsf{K}_\nabla(\boldsymbol{\theta}) + \eta_{\mathsf{K}_\nabla}\mathsf{I}) \leq \kappa_{\max}$ when $\boldsymbol{\theta} = \theta\mathbf{1}$, we can see that in practice the condition number of the covariance matrix is smaller than $\kappa_{\max}$ when $\boldsymbol{\theta} = \theta\mathbf{1}$ and once again for most of the plotted domain of $\boldsymbol{\theta}$. By having $\rho > 1$ we lose the proven bound on the condition number of K_∇. However, as was shown in Fig. 10b, having a smaller $v_{\min}$ reduces the difference between the gradient of the surrogate and of the function of interest. Section 10.6 demonstrates that having $\rho > 1$ is advantageous for optimization.

10.4 Non-isotropic rescaling of X

It is common to either not rescale the data or to do so such that all of the data points are in a unit cube [3]. For the method presented in this paper the data is rescaled to ensure $v_{\min} = v_{\min,\text{set}}$, where $v_{\min,\text{set}}$ comes from either Eq. (66) or Eq. (67). In this section we demonstrate how an iterative non-isotropic rescaling can be used to also ensure that $\|\boldsymbol{\theta} - \theta\mathbf{1}\| < \epsilon$, where ϵ is set to a small positive value such as 10^{-2}. This is important since the results from Sections 8 and 9 only ensure $\kappa(\mathsf{K}_\nabla(\boldsymbol{\theta}) + \eta_{\mathsf{K}_\nabla}\mathsf{I}) \leq \kappa_{\max}$ when $\boldsymbol{\theta} = \theta\mathbf{1}$. When the marginal log-likelihood is first maximized it is likely that $\boldsymbol{\theta} \neq \theta\mathbf{1}$. However, the non-isotropic rescaling is used such that when the marginal log-likelihood is maximized again with the scaled data , the result is $\boldsymbol{\theta} \approx \theta\mathbf{1}$. This iterative process of non-isotropically rescaling the data and maximizing the marginal log-likelihood is repeated until $\|\boldsymbol{\theta} - \theta\mathbf{1}\| < \epsilon$. As is shown in this section, this may require 2-4 iterations, depending on the selected value of ϵ.

It is straightforward to demonstrate that the closest point on the line $\theta\mathbf{1}$ to $\boldsymbol{\theta}$ is when $\theta = \alpha$, where

$$\alpha = \frac{\boldsymbol{\theta}^T\mathbf{1}}{d}. \tag{68}$$

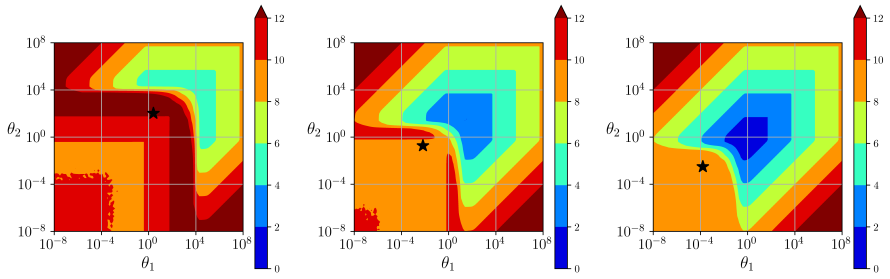

(a) $n_x = 10$ and $v_{\min} = 0.01$ (b) $n_x = 10$ and $v_{\min} = \frac{2\sqrt{d}}{10} \approx 0.283$ (c) $n_x = 10$ and $v_{\min} = 2\sqrt{d}$

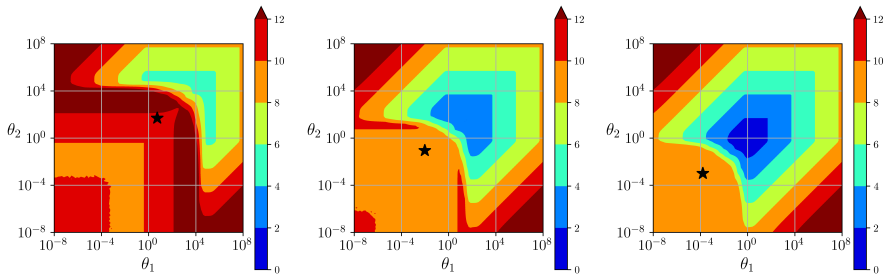

(d) $n_x = 50$ and $v_{\min} = 0.01$ (e) $n_x = 50$ and $v_{\min} = \frac{2\sqrt{d}}{10} \approx 0.283$ (f) $n_x = 50$ and $v_{\min} = 2\sqrt{d}$

Fig. 11: Plots of $\kappa\left(\mathsf{K}_\nabla(\boldsymbol{\theta}) + \eta_{\mathsf{K}_\nabla}\mathsf{I}\right)$ with $d = 2$, and $\eta_{\mathsf{K}_\nabla} = \eta_{\mathsf{K}}$ from Eq. (16). Regions where $\kappa\left(\mathsf{K}_\nabla(\boldsymbol{\theta}) + \eta_{\mathsf{K}_\nabla}\mathsf{I}\right) \geq \kappa_{\max} = 10^{10}$ are in red and the location where the marginal likelihood from Eq. (12) is maximized is indicated by a star marker.

The Euclidean distance between $\alpha\mathbf{1}$ and $\boldsymbol{\theta}$ is

$$\begin{aligned}\delta_{\min}(\boldsymbol{\theta}) &= \|\boldsymbol{\theta} - \alpha\mathbf{1}\|_2 \\ &= \boldsymbol{\theta}^T\boldsymbol{\theta} - \frac{\left(\boldsymbol{\theta}^T\mathbf{1}\right)^2}{d}.\end{aligned} \tag{69}$$

The goal is to rescale X non-isotropically with the vector $\boldsymbol{\gamma}$ such that $\boldsymbol{\theta} = \alpha\mathbf{1}$. From Eq. (1) we have

$$\begin{aligned}e^{-\sum_{i=1}^d \theta_i\left(x^{(i)} - y^{(i)}\right)^2} &= e^{-\sum_{i=1}^d \alpha\left(\gamma_i x^{(i)} - \gamma_i y^{(i)}\right)^2} \\ \gamma_i &= \sqrt{\frac{\theta_i}{\alpha}}.\end{aligned} \tag{70}$$

We can thus rescale X and F_∇ with

$$\mathsf{X}_{\text{new}} = \mathsf{X}\,\Gamma \tag{71}$$

$$\mathsf{F}_{\nabla,\text{new}} = \mathsf{F}_\nabla\,\Gamma^{-1}, \tag{72}$$

where $\mathit{\Gamma} = \mathrm{diag}(\boldsymbol{\gamma})$. After the non-isotropic rescaling both X_{new} and $\mathsf{F}_{\nabla,\mathrm{new}}$ still need to be rescaled isotropically to ensure $v_{\mathrm{min}} = v_{\mathrm{min,set}}$ since the shortest Euclidean distance between data points is likely to have changed from the non-isotropic rescaling. Furthermore, this isotropic rescaling cannot be done a priori since the two points with the shortest Euclidean distance may change from the non-isotropic scaling. Algorithm 1 provides the steps to implement the non-isotropic rescaling. The initial data can be recovered from the scaled data with

$$\mathsf{X}_{\mathrm{init}} = \mathsf{X}_{\mathrm{final}}\, \mathit{\Gamma}_{\mathrm{final}}^{-1} \tag{73}$$

$$\mathsf{F}_{\nabla,\mathrm{init}} = \mathsf{F}_{\nabla,\mathrm{final}}\, \mathit{\Gamma}_{\mathrm{final}} \tag{74}$$

$$\mathit{\Gamma}_{\mathrm{final}} = \left(\prod_{k=0}^{n_k} \tau^{(k)}\right)\left(\prod_{k=1}^{n_k} \mathit{\Gamma}^{(k)}\right), \tag{75}$$

where the superscript in parentheses indicates the iteration counter for the scaling in Algorithm 1, and n_k is the total number of iterations. When $\boldsymbol{\theta}$ is set by maximizing the marginal log-likelihood without iteratively rescaling the data, the entries in the vector $\boldsymbol{\theta}$ are the inverse of the squared characteristic lengths. When the iterative non-isotropic rescaling method is used, we have $\boldsymbol{\theta} \approx \theta\mathbf{1}$. The inverse characteristic lengths are thus not found in $\boldsymbol{\theta}$, but instead along the diagonal of the rescaling matrix $\mathit{\Gamma}_{\mathrm{final}}$.

Algorithm 1 Isotropic ($k_{\max} = 0$) and non-isotropic ($k_{\max} > 0$) rescaling of X and F_{∇}

Require: $n_x > 1$, $v_{\mathrm{min,init}} > 0$, and user-set $\epsilon \geq 0$
  Set $k = 0$ and calculate $v_{\mathrm{min,init}}$ from $\mathsf{X}_{\mathrm{init}}$
  $\tau^{(0)} = \frac{v_{\mathrm{min,set}}}{v_{\mathrm{min,init}}}$
  $\mathsf{X}^{(0)} = \tau^{(0)}\mathsf{X}_{\mathrm{init}}$
  $\mathsf{F}_{\nabla}^{(0)} = \frac{\mathsf{F}_{\nabla,\mathrm{init}}}{\tau^{(0)}}$
  Solve Eq. (12) for $\bar{\boldsymbol{\theta}}$
  $\alpha = \frac{\bar{\theta}^T\mathbf{1}}{d}$
  $\delta_{\mathrm{min}} = \bar{\boldsymbol{\theta}}^T\bar{\boldsymbol{\theta}} - \frac{\left(\bar{\boldsymbol{\theta}}^T\mathbf{1}\right)^2}{d}$
  while $\delta_{\mathrm{min}} > \epsilon$ and $k \leq k_{\max}$ **do**
    $k = k + 1$
    $\mathit{\Gamma}^{(k)} = \mathrm{diag}\left(\sqrt{\frac{\bar{\boldsymbol{\theta}}}{\alpha}}\right)$
    $\mathsf{X}_{\mathrm{init}}^{(k)} = \mathsf{X}^{(k-1)}\mathit{\Gamma}^{(k)}$ (update $v_{\mathrm{min,init}}$)
    $\tau^{(k)} = \frac{v_{\mathrm{min,set}}}{v_{\mathrm{min,init}}^{(k)}}$
    $\mathsf{X}^{(k)} = \tau^{(k)}\mathsf{X}_{\mathrm{init}}^{(k)}$
    $\mathsf{F}_{\nabla}^{(k)} = \frac{\mathsf{F}_{\nabla}^{(k-1)}\left(\mathit{\Gamma}^{(k)}\right)^{-1}}{\tau^{(k)}}$
    Solve Eq. (12) with the initial solution $\mathbf{1}\frac{\alpha}{\left(\tau^{(k)}\right)^2}$ for $\bar{\boldsymbol{\theta}}$
    Updates δ_{min} and α
  end while

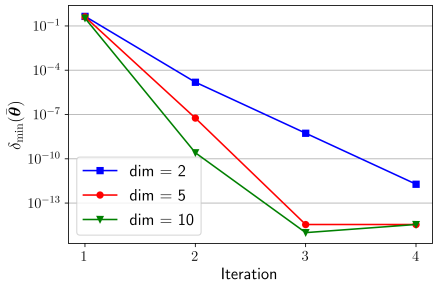

Fig. 12: Convergence of $\bar{\boldsymbol{\theta}}$ to $\theta\mathbf{1}$ using the iterative non-isotropic rescaling of X from Algorithm 1, where $\delta_{v_{\min}}(\bar{\boldsymbol{\theta}})$ is calculated with Eq. (69).

To demonstrate how the non-isotropic rescaling works in practice, a matrix X was created with a Latin hypercube sampling, $n_x = 10$, the domain $[-1, 1]^d$, and $d \in \{2, 5, 10\}$. Eq. (20) and its gradient were evaluated at all the rows in X and Eq. (67) was used to calculate $v_{\min,\text{set}}$ with $\rho = 1$. Algorithm 1 was then used with $\epsilon = 0$ and $k_{\max} = 3$. Fig. 12 shows how the non-isotropic scaling allows the solution of Eq. (12) to quickly converge to $\theta\mathbf{1}$. This ensures that the bounds on the condition number of the covariance matrix apply even when the initial solution to Eq. (12) is far from $\theta\mathbf{1}$.

10.5 Steps for ensuring $\kappa\left(\mathsf{K}_\nabla(\theta) + \eta_{\mathsf{K}_\nabla}\mathsf{I}\right) \leq \kappa_{\max}$

The five steps provided in this subsection provide a non-intrusive method of ensuring the gradient-enhanced covariance matrix has a condition number below $\kappa_{\max}$. If $\rho = 1$ and the non-isotropic rescaling of X is used, then the constraint in Eq. (12) for the condition number of the covariance matrix will not be active. When $\rho > 1$, the constraint in Eq. (12) may be active even with the non-isotropic rescaling of X. However, it was found that when a modest value of ρ was used, such as $\rho = 10$, then the non-isotropic rescaling of X from Algorithm 1 was sufficient to ensure the condition number of the gradient-enhanced covariance matrix has a condition number below $\kappa_{\max}$ without having an active constraint in Eq. (12). Furthermore, as is demonstrated in Section 10.6, using $\rho > 1$ allows a Bayesian optimizer to achieve more rapid convergence of the optimality relative to the case with $\rho = 1$. As was detailed in Section 10.2, having a larger $v_{\min,\text{set}}$ leads to larger difference between the gradient of the surrogate and of the function of interest. Therefore, by having $\rho > 1$, $v_{\min,\text{set}}$ is smaller and thus the surrogate is more accurate. The suggested value for ϵ is 10^{-2}. From Fig. 12, it is clear that ϵ can be selected to be significantly smaller, such as 10^{-10}. However, selecting a smaller ϵ requires additional iterations that involve optimizing the hyperparameters $\boldsymbol{\theta}$ several times.

1. Use suggested parameters or modify as desired
   (a) $\kappa_{\max} = 10^{10}$

   (b) $\rho = 1$ for proven bound on the condition number or $\rho = 10$ for efficient optimization
   (c) $k_{\max} = 0$ for isotropic rescaling of X or $k_{\max} = 3$ and $\epsilon = 10^{-2}$ for non-isotropic rescaling of X
2. Calculate the following parameters
   (a) $v_{\min,\text{set}}$ using Eq. (67), or alternatively Eq. (66)
   (b) η_{K_∇} with Eq. (65) using $v_{\min} = \rho v_{\min,\text{set}}$
3. Use Algorithm 1 to rescale X and F_∇, and to solve for the hyperparameter $\boldsymbol{\theta}$
4. Evaluate the surrogate with Eqs. (9) and (10)
5. Unscale the data using Eqs. (73) and (74)

10.6 Bayesian optimization test case

As is apparent in Fig. 1, the ill-conditioning problem for the gradient-enhanced covariance matrix becomes more acute as the data points get closer together. This will naturally happen when there is a larger number of data points and when the data points are selected to be close together. This may be done, for example, to reduce the surrogate's uncertainty in a given region of the parameter space, or to achieve deep convergence for Bayesian optimization. As such, to highlight the ability of the method from this paper to overcome the ill-conditioning of the gradient-enhanced covariance matrix a local optimization test case is used. The goal of this test case is to highlight how this method overcomes the ill-conditioning problem for the gradient-enhanced covariance matrix and thus allows for deeper convergence to be achieved. While the test case is for local optimization, this method can also be applied with a gradient-enhanced GP for any other use such as for global Bayesian optimization, uncertainty quantification, or classification.

Minimizations of the unimodal Rosenbrock function from Eq. (20) with $d = 2$ and $d = 5$ were performed first without rescaling X and then repeated using the steps in Section 10.5 with $\rho = 1$ and $\rho = 10$. A simple acquisition function is the upper-confidence bound

$$h(\boldsymbol{x}) = \mu_f(\boldsymbol{x}) - \omega\sigma_f(\boldsymbol{x}), \tag{76}$$

where a large value for ω promotes exploration while a small value promotes exploitation. Since we were interested in local optimization and achieving deep convergence, we used $\omega = 0$.

For all test cases the optimizer was started with the initial solution at $\boldsymbol{x} = [2, \ldots, 2]^T$. All subsequent points were selected by minimizing the acquisition function. A gradient-based optimizer was used to maximize the marginal log-likelihood from Eq. (12) and to minimize the acquisition function. Since these functions can be multimodal, the optimizers were started with five initial points using a Latin hypercube sampling. A baseline method that does not rescale the data points was used to compare with the method presented in this paper. For the baseline method $\eta_{\mathsf{K}_\nabla} = \eta_{\mathsf{K}}$ from Eq. (16) was used.

It was not possible for the baseline method to be non-regularized, i.e. to use $\eta_{\mathsf{K}_\nabla} = 0$, since for most values of $\boldsymbol{\theta}$ this resulted in the failure of the Cholesky decomposition for the gradient-enhanced covariance matrix due to its severe ill-conditioning.

Figs. 13a and 13d show the convergence history when X is not rescaled. For both the $d = 2$ and $d = 5$ cases, the optimizer stalls when the optimality and the Euclidean distance to the minimum reach approximately 10^{-5}. The optimizer stalls since the solution $\bar{\boldsymbol{\theta}}$ from Eq. (12) is highly restricted by the constraint on the condition number, as shown in Fig. 11. As a consequence of ensuring the constraint is satisfied, $\bar{\boldsymbol{\theta}}$ does not provide a large marginal likelihood and thus the surrogate is not an effective approximation to the function of interest.

Figs. 13c and 13f show the convergence of the optimizer when X is rescaled using Eq. (67) with $\rho = 1$. In this case the results from Sections 8 and 9 and the non-isotropic rescaling of X ensure that $\kappa(\mathsf{K}_\nabla(\boldsymbol{\theta}) + \eta_{\mathsf{K}_\nabla}\mathsf{I}) \leq \kappa_{\max}$. For the $d = 2$ case the optimizer is able to converge the optimality an additional four orders of magnitude relative to the cases when X is not rescaled. However, comparing Figs. 13a and 13c we see that the rescaling method slows down the initial convergence and this also holds for the $d = 5$ case. This slower convergence is due to the larger size of $v_{\min}$, which increases the difference between the gradient of the surrogate and of the function of interest, as explained in 10.2.

For the optimization in Figs. 13b and 13e, the steps from Section 10.5 were used with $\rho = 10$. For the $d = 2$ case the optimizer converges nearly as deeply as the case with the rescaling with $\rho = 1$ and achieves deeper convergence when $d = 5$. For both the $d = 2$ and $d = 5$ cases the optimizer convergences as fast as the non-rescaled case and significantly faster than the case with rescaling and $\rho = 1$. In fact, for the $d = 5$ case the optimizer with $\rho = 10$ gets to within a distance of 10^{-9} of the solution after 40 iterations while the optimizer with $\rho = 1$ does not achieve this level of convergence after 60 iterations.

By increasing $v_{\min}$ the condition number of the covariance matrix is reduced, which ensures the solution to Eq. (12) is not limited by the constraint on the condition number. However, the trade-off to increasing $v_{\min}$ is that this increases the difference between the gradient of the surrogate and of the function of interest, as detailed in Section 10.2 and demonstrated in Fig. 13. The use of Algorithm 1 with $\rho = 10$ was found to provide a good balance and an efficient optimizer that is able to achieve deep and rapid convergence.

11 Conclusions

The ill-conditioning of the gradient-enhanced covariance matrix has been extensively studied and various methods have been proposed. Unfortunately, these previous methods require undesirable trade-offs such as removing certain data points and setting a minimum Euclidean distance between data points. Furthermore, none of the prior methods guaranteed an upper bound on the condition number of the gradient-enhanced covariance matrix.

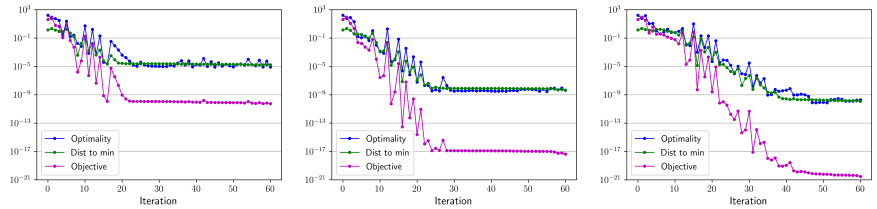

(a) $d = 2$, $v_{\min} = v_{\min,\text{init}}$, and $\eta_{\mathsf{K}_\nabla} = \eta_{\mathsf{K}}$

(b) $d = 2$, $v_{\min} = v_{\min,\text{set}}$, $\eta_{\mathsf{K}_\nabla} = \eta_{\mathsf{K}_\nabla}(\rho \cdot v_{\min,\text{set}})$, and $\rho = 10$

(c) $d = 2$, $v_{\min} = v_{\min,\text{set}}$, $\eta_{\mathsf{K}_\nabla} = \eta_{\mathsf{K}_\nabla}(\rho \cdot v_{\min,\text{set}})$, and $\rho = 1$

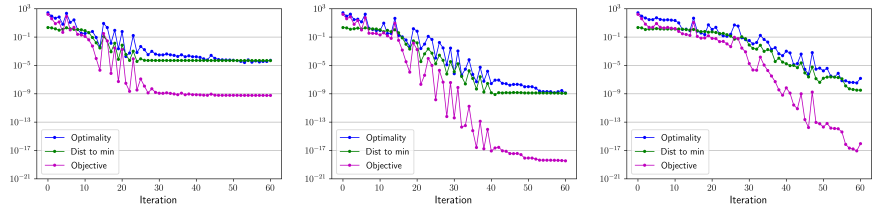

(d) $d = 5$, $v_{\min} = v_{\min,\text{init}}$, and $\eta_{\mathsf{K}_\nabla} = \eta_{\mathsf{K}}$

(e) $d = 5$, $v_{\min} = v_{\min,\text{set}}$, $\eta_{\mathsf{K}_\nabla} = \eta_{\mathsf{K}_\nabla}(\rho \cdot v_{\min,\text{set}})$, and $\rho = 10$

(f) $d = 5$, $v_{\min} = v_{\min,\text{set}}$, $\eta_{\mathsf{K}_\nabla} = \eta_{\mathsf{K}_\nabla}(\rho \cdot v_{\min,\text{set}})$, and $\rho = 1$

Fig. 13: Optimization test case using the Rosenbrock function from Eq. (20), $\kappa_{\max} = 10^{10}$, Eqs. (16) and (65) for η_{K} and η_{K_∇}, respectively, and Eq. (67) is used to calculate $v_{\min,\text{set}}$.

In the method presented in this paper, the matrix of data points is rescaled such that the minimum Euclidean distance between data points is sufficiently large. This simple method is non-intrusive since it only requires the matrix of data points X and the matrix of gradients F_∇ to be rescaled and for a modest nugget to be used. A simple algebraic equation was derived to calculate the minimum required Euclidean distance to rescale X along with a modest nugget value. The procedure is detailed in Section 10.5. The method presented in this paper is advantageous since it is easy to implement, all data points can be kept, deep and rapid convergence can be achieved, and the condition number is bounded below a user-set threshold. This was demonstrated in Section 10.6 where the two and five dimensional Rosenbrock function was minimized without any ill-conditioning of the covariance matrix. Furthermore, the method presented in this paper allowed the optimizer to converge the optimality an additional four orders of magnitude relative to the standard method without rescaling.

Acknowledgements The authors would like to thank Prof. Prasanth Nair and Prof. Masayuki Yano for helpful discussions that helped improve this paper. The authors would also like to acknowledge financial support provided by the Natural Sciences and Engineering Research Council of Canada and the Ontario Graduate Scholarship Program.

References

1. Ababou, R., Bagtzoglou, A.C., Wood, E.F.: On the condition number of covariance matrices in kriging, estimation, and simulation of random fields. Mathematical Geology **26**(1), 99–133 (1994). DOI 10.1007/BF02065878
2. Andrianakis, I., Challenor, P.G.: The effect of the nugget on Gaussian process emulators of computer models. Computational Statistics & Data Analysis **56**(12), 4215–4228 (2012). DOI 10.1016/j.csda.2012.04.020
3. Dalbey, K.: Efficient and robust gradient enhanced Kriging emulators. Tech. Rep. SAND2013-7022, 1096451 (2013). DOI 10.2172/1096451
4. Davis, G.J., Morris, M.D.: Six Factors Which Affect the Condition Number of Matrices Associated with Kriging. Mathematical Geology **29**(5), 669–683 (1997). DOI 10.1007/BF02769650
5. Dwight, R., Han, Z.H.: Efficient Uncertainty Quantification Using Gradient-Enhanced Kriging. In: 11th AIAA Non-Deterministic Approaches Conference. American Institute of Aeronautics and Astronautics, Palm Springs, California (2009). DOI 10.2514/6.2009-2276
6. Eriksson, D., Dong, K., Lee, E., Bindel, D., Wilson, A.G.: Scaling Gaussian Process Regression with Derivatives. In: 32nd Conference on Neural Information Processing Systems. Montreal, Canada (2018)
7. Gramacy, R.B., Lee, H.K.H.: Cases for the nugget in modeling computer experiments. Statistics and Computing **22**(3), 713–722 (2012). DOI 10.1007/s11222-010-9224-x
8. Han, Z.H., Görtz, S., Zimmermann, R.: Improving variable-fidelity surrogate modeling via gradient-enhanced kriging and a generalized hybrid bridge function. Aerospace Science and Technology **25**(1), 177–189 (2013). DOI 10.1016/j.ast.2012.01.006
9. He, X., Chien, P.: On the Instability Issue of Gradient-Enhanced Gaussian Process Emulators for Computer Experiments. SIAM/ASA Journal on Uncertainty Quantification **6**(2), 627–644 (2018). DOI 10.1137/16M1088247
10. Huang, D., Tang, Y., Zhang, W.: Distribution of roots of cubic equations. The Pure and Applied Mathematics **17**(2), 185–188 (2010)
11. Kostinski, A.B., Koivunen, A.C.: On the condition number of Gaussian sample-covariance matrices. IEEE Transactions on Geoscience and Remote Sensing **38**(1), 329–332 (2000). DOI 10.1109/36.823928
12. Laurent, L., Le Riche, R., Soulier, B., Boucard, P.A.: An Overview of Gradient-Enhanced Metamodels with Applications. Archives of Computational Methods in Engineering **26**(1), 61–106 (2019). DOI 10.1007/s11831-017-9226-3
13. March, A., Willcox, K., Wang, Q.: Gradient-based multifidelity optimisation for aircraft design using Bayesian model calibration. The Aeronautical Journal **115**(1174), 729–738 (2011). DOI 10.1017/S0001924000006473
14. Ollar, J., Mortished, C., Jones, R., Sienz, J., Toropov, V.: Gradient based hyper-parameter optimisation for well conditioned kriging metamodels. Structural and Multidisciplinary Optimization **55**(6), 2029–2044 (2017). DOI 10.1007/s00158-016-1626-8
15. Osborne, M.A., Garnett, R., Roberts, S.J.: Gaussian Processes for Global Optimization. In: 3rd International Conference on Learning and Intelligent Optimization. Trento, Italy (2009)
16. Rasmussen, C.E., Williams, C.K.I.: Gaussian Processes for Machine Learning. Adaptive Computation and Machine Learning. MIT Press, Cambridge, Mass (2006)
17. Riley, J.D.: Solving Systems of Linear Equations With a Positive Definite, Symmetric, but Possibly Ill-Conditioned Matrix. Mathematical tables and other aids to computation pp. 96–101 (1955)
18. Schulz, E., Speekenbrink, M., Krause, A.: A tutorial on Gaussian process regression: Modelling, exploring, and exploiting functions. Journal of Mathematical Psychology **85**, 1–16 (2018). DOI 10.1016/j.jmp.2018.03.001
19. Selby, S.M.: CRC Standard Mathematical Tables, twenty-third edn. CRC Press, Cleveland, Ohio (1975)
20. Shahriari, B., Swersky, K., Wang, Z., Adams, R.P., de Freitas, N.: Taking the Human Out of the Loop: A Review of Bayesian Optimization. Proceedings of the IEEE **104**(1), 148–175 (2016). DOI 10.1109/JPROC.2015.2494218

21. Toal, D.J., Bressloff, N.W., Keane, A.J., Holden, C.M.: The development of a hybridized particle swarm for kriging hyperparameter tuning. Engineering Optimization **43**(6), 675–699 (2011). DOI 10.1080/0305215X.2010.508524
22. Toal, D.J.J., Bressloff, N.W., Keane, A.J.: Kriging Hyperparameter Tuning Strategies. AIAA Journal **46**(5), 1240–1252 (2008). DOI 10.2514/1.34822
23. Toal, D.J.J., Forrester, A.I.J., Bressloff, N.W., Keane, A.J., Holden, C.: An adjoint for likelihood maximization. Proceedings of the Royal Society A: Mathematical, Physical and Engineering Sciences **465**(2111), 3267–3287 (2009). DOI 10.1098/rspa.2009.0096
24. Wu, A., Aoi, M.C., Pillow, J.W.: Exploiting gradients and Hessians in Bayesian optimization and Bayesian quadrature. arXiv:1704.00060 [stat] (2018)
25. Wu, J., Poloczek, M., Wilson, A.G., Frazier, P.: Bayesian Optimization with Gradients. In: 31st Conference on Neural Information Processing Systems. Long Beach, CA, USA (2017)
26. Zhang, Y., Leithead, W.E.: Exploiting Hessian matrix and trust-region algorithm in hyperparameters estimation of Gaussian process. Appl. Math. Comput. p. 18 (2005)
27. Zimmermann, R.: On the Maximum Likelihood Training of Gradient-Enhanced Spatial Gaussian Processes. SIAM Journal on Scientific Computing **35**(6), A2554–A2574 (2013). DOI 10.1137/13092229X
28. Zimmermann, R.: On the condition number anomaly of Gaussian correlation matrices. Linear Algebra and its Applications **466**, 512–526 (2015). DOI 10.1016/j.laa.2014.10.038
29. Zingg, D.W., Nemec, M., Pulliam, T.H.: A comparative evaluation of genetic and gradient-based algorithms applied to aerodynamic optimization. European Journal of Computational Mechanics **17**(1-2), 103–126 (2008). DOI 10.3166/remn.17.103-126

12 Proofs for Section 7

12.1 Proof of Proposition 6

The results from the two following lemmas prove that $v_a^*(\theta, d)$ is monotonically decreasing with respect to θ and monotonically increasing with respect to d.

Lemma 13 *For $\theta > 0$ and $d \in \mathbb{Z}^+$, the function $v_a^*(\theta; d)$ is monotonically decreasing with respect to θ.*

Proof Consider the derivative of $v_a^*(\theta)$ with respect to θ:

$$\frac{\partial v_a^*(\theta)}{\partial \theta} = \frac{\sqrt{1+8\theta d} - (1+4\theta d)}{4\theta^2 \sqrt{d}\sqrt{1+8\theta d}}, \tag{77}$$

where it is clear that the denominator is always positive for $d \in \mathbb{Z}^+$ and $\theta > 0$. We begin by assuming that the numerator is negative and show that this holds for $d \in \mathbb{Z}^+$ and $\theta > 0$:

$$\begin{aligned} \sqrt{1+8\theta d} - (1+4\theta d) &< 0 \\ \left(\sqrt{1+8\theta d}\right)^2 &< (1+4\theta d)^2 \\ -16\theta^2 d^2 &< 0, \end{aligned}$$

where both sides of the inequality on the second line are positive prior to being squared for $d \in \mathbb{Z}^+$ and $\theta > 0$. As such, the squaring operation does not change their respective signs or the direction of the inequality. Since the denominator of $\frac{\partial v_a^*(\theta)}{\partial \theta}$ is always positive and its numerator is negative, it follows that $v_a^*(\theta)$ is monotonically decreasing with respect to θ, which completes the proof.

Lemma 14 *The function $v_a^*(\theta; d)$ is monotonically increasing with respect to d for $d \in \mathbb{Z}^+$ and $\theta > 0$.*

Proof We have $d \in \mathbb{Z}^+$ but for this analysis we consider d to be a continuous variable and we calculate the derivative of $v_a^*(d)$ with respect to d:

$$\frac{\partial v_a^*(d)}{\partial d} = \frac{\sqrt{1+8\theta d}-1}{8\theta d^{\frac{3}{2}}\sqrt{1+8\theta d}}. \tag{78}$$

Both the numerator and denominator are always positive for $\theta > 0$ and $d > 0$. Consequently, $v_a^*(d)$ is monotonically increasing for $d > 0$.

The two following lemmas bound $v_a^*(\theta; d)$ by using the result from Lemmas 13 and 14.

Lemma 15 *For $\theta > 0$ and $d \in \mathbb{Z}^+$, the supremum of $v_a^*(\theta; d)$ is $\sqrt{d}$ at $\theta = 0$.*

Proof As a consequence of Lemma 13, v_a^* is maximized when θ is minimized. We thus evaluate $\lim_{\theta\to 0} v_a^*(\theta)$ using L'Hôpital's rule:

$$\begin{aligned}\lim_{\theta\to 0} v_a^*(\theta; d) &= \lim_{\theta\to 0} \frac{-1+\sqrt{1+8\theta d}}{4\theta\sqrt{d}} \\ &= \lim_{\theta\to 0} \frac{4d\,(1+8\theta d)^{-\frac{1}{2}}}{4\sqrt{d}} \\ &= \sqrt{d},\end{aligned}$$

which is the desired result.

Lemma 16 *We have $v_a^*(\theta; d) \leq \frac{1}{\sqrt{2\theta}}$ for $\theta > 0$ and $d \in \mathbb{Z}^+$.*

Proof From Lemma 14 we know that $v_a^*(\theta; d)$ is monotonically increasing for $d > 0$. As such, we can derive an upper bound on $v_a^*(\theta; d)$ by considering the following limit:

$$\begin{aligned}u_{v_a^*}(\theta) &= \lim_{d\to\infty} v_a^*(\theta; d) \\ &= \lim_{d\to\infty} \frac{-\frac{1}{\sqrt{d}} + \sqrt{\frac{1}{d}+8\theta}}{4\theta} \\ &= \frac{1}{\sqrt{2\theta}},\end{aligned}$$

which completes the proof.

We have shown that $v_a^*(\theta; d) \leq \sqrt{d}$ and $v_a^*(\theta; d) \leq \frac{1}{\sqrt{2\theta}}$. We therefore have $v_a^*(\theta; d) \leq \min\left(\sqrt{d}, \frac{1}{\sqrt{2\theta}}\right)$, which completes the proof of Proposition 6.

12.2 Proof of Proposition 9

To identify the maximum of u_{r_b} we begin by calculating its derivative:

$$\frac{\partial u_{r_b}(v_b)}{\partial v_b} = -2\theta(n_x-1)\left[4\theta^2\sqrt{d}v_b^3 + 2\theta v_b^2 - 4\theta\sqrt{d}v_b - 1\right]e^{-\theta v_b^2}, \tag{79}$$

which is zero if the following cubic is satisfied:

$$v_b^3 + \frac{1}{2\theta\sqrt{d}}v_b^2 - \frac{1}{\theta}v_b - \frac{1}{4\theta^2\sqrt{d}} = 0. \tag{80}$$

A general cubic equation is $v^3 + a_2v^2 + a_1v + a_0 = 0$ where we have $a_2 = \frac{1}{2\theta\sqrt{d}}$, $a_1 = -\frac{1}{\theta}$, and $a_0 = -\frac{1}{4\theta^2\sqrt{d}}$. We can determine if the cubic equation has one or three real roots by checking the sign of the discriminant [10], which is given by

$$\begin{aligned}\Delta &= \frac{4a_2^3a_0 - a_2^2a_1^2 + 4a_1^3 - 18a_2a_1a_0 + 27a_0^2}{108}\\ &= -\frac{64\theta^2d^2 + 13\theta d + 2}{1728\,\theta^5d^2},\end{aligned} \tag{81}$$

which is negative for $\theta > 0$ and $d \in \mathbb{Z}^+$. A negative discriminant indicates the cubic equation has three real roots [10]. Furthermore, for $d \in \mathbb{Z}^+$ and $\theta > 0$, we have $a_2 > 0$, $a_0 < 0$, which is Case III3 in the first table in [10]. Case III3 indicates that only one of the three roots is positive and the other two are negative. We use the cubic solution from [19] to calculate the only positive root of Eq. (80):

$$v_b^* = \frac{\sqrt{12d\theta+1}}{3\theta\sqrt{d}}\cos\left(\frac{1}{3}\cos^{-1}\left(\frac{9d\theta-1}{(12d\theta+1)^{\frac{3}{2}}}\right)\right) - \frac{1}{6\theta\sqrt{d}},$$

which matches Eq. (44) and this completes the proof.

12.3 Proof of Lemma 2

Consider the following reformulation of $u_{r_b}(v_b)$:

$$\begin{aligned}u_{r_b}(v_b) &= 2\theta v_b(n_x-1)\left(1 + 2\theta\sqrt{d}\,v_b\right)e^{-\theta v_b^2}\\ &= \underbrace{2\theta v_b(n_x-1)e^{-\theta v_b^2}}_{u_{r_b,1}(v_b)} + \underbrace{4\theta^2v_b^2\sqrt{d}(n_x-1)e^{-\theta v_b^2}}_{u_{r_b,2}(v_b)}.\end{aligned}$$

The positive root for the gradient of $u_{r_b,1}(v_b)$ is

$$\begin{aligned}\frac{\partial u_{r_b,1}(v_b)}{\partial v_b} &= 2\theta(n_x-1)\left[1 - 2\theta v_b^2\right]e^{-\theta v_b^2} = 0\\ v_{b1}^*(\theta) &= \frac{1}{\sqrt{2\theta}},\end{aligned} \tag{82}$$

and analogously for $u_{r_b,2}(v_b)$ we find its unique positive critical point is $v^*_{b2}(\theta) = \frac{1}{\sqrt{\theta}}$, which match Eqs. (45) and (46), respectively. It is straightforward to check that both v^*_{b1} and v^*_{b2} are the location of the maximum for $u_{r_b,1}(v_b)$ and $u_{r_b,2}(v_b)$, respectively. Both $\frac{\partial u_{r_b,1}(v_b)}{\partial v_b}$ and $\frac{\partial u_{r_b,2}(v_b)}{\partial v_b}$ are positive when $v < v^*_{b1}$, and both are negative when $v > v^*_{b2}$. Therefore, $\frac{\partial u_{r_b}(v_b)}{\partial v_b}$ can only be zero in the range $v^*_{b1}(\theta) = \frac{1}{\sqrt{2\theta}} < v^*_b(\theta) < \frac{1}{\sqrt{\theta}} = v^*_{b2}(\theta)$. We therefore have $\ell_{v^*_b}(\theta) = v^*_{b1}(\theta) = \frac{1}{\sqrt{2\theta}}$ and $u_{v^*_b}(\theta) = v^*_{b2}(\theta) = \frac{1}{\sqrt{\theta}}$, which completes the proof of Lemma 2.

12.4 Proof of Lemma 4

We need to derive $\ell_{\theta^*_b}(v_{\min})$ and $u_{\theta^*_b}(v_{\min})$ and prove that $u_{\hat{\theta}_b} < \ell_{\theta^*_b}$ for $d \in \mathbb{Z}^+$ and $v_{\min} > 0$. We begin by showing that $\theta^*_b(d)$ from Eq. (43) is monotonically increasing with respect to d:

$$\frac{\partial \theta^*_b}{\partial d} = \frac{\sqrt{v^2_{\min} + 16d} - v_{\min}}{8d^{\frac{3}{2}} v_{\min} \sqrt{v^2_{\min} + 16d}}, \tag{83}$$

which is always positive for $d \in \mathbb{Z}^+$ and $v_{\min} > 0$. Lower and upper bounds on $\theta^*_b(d)$ are thus given by

$$\ell_{\theta^*_b} = \theta^*_b(d = 1) \ = \frac{1}{v^2_{\min}} + \frac{\sqrt{v^2_{\min} + 16} - v_{\min}}{4v^2_{\min}} \tag{84}$$

$$u_{\theta^*_b} = \lim_{d \to \infty} \theta^*_b(d) \leq \frac{2}{v^2_{\min}}. \tag{85}$$

Comparing $u_{\hat{\theta}_b}(v_{\min}) = \frac{1}{v^2_{\min}}$ from Eq. (48) and $\ell_{\theta^*_b}(v_{\min})$ from Eq. (49) it is clear that $u_{\hat{\theta}_b}(v_{\min}) < \ell_{\theta^*_b}(v_{\min})$ for $v_{\min} > 0$. We thus have $\hat{\theta}_b < u_{\hat{\theta}_b} < \ell_{\theta^*_b} \leq \theta^*_b < u_{\theta^*_b}$, which completes the proof of Lemma 4.

12.5 Proof of Lemma 7

We start by considering the limit $\lim_{\theta \to 0} u_{r_a}$. From Proposition 6 we have $v^*_a \leq \sqrt{d}$ and therefore $v_a(\theta) = \min(v_{\min}, \sqrt{d})$. Our limit of interest is given by

$$\begin{aligned} \lim_{\theta \to 0} u_{r_a}(\theta, v_a(\theta)) &= \lim_{\theta \to 0} (n_x - 1) \left(1 + 2\theta\sqrt{d} v_a(\theta)\right) e^{-\theta v^2_a(\theta)} \\ &= n_x - 1, \end{aligned}$$

which is the desired result. We next consider the limit $\lim_{\theta \to 0} u_{r_b}$. From Lemma 2 we have $\frac{1}{\sqrt{2\theta}} = \ell_{v^*_b}(\theta) < v^*_b(\theta) < u_{v^*_b}(\theta)) = \frac{1}{\sqrt{\theta}}$. Therefore, we

have $v_b^*(\theta \to 0) \to \infty$ and thus, $v_b(\theta \to 0) = v_b^*$. However, we also have the following relations:

$$\lim_{\theta\to 0} \theta \ell_{v_b^*}(\theta) = \lim_{\theta\to 0} \sqrt{\frac{\theta}{2}} = 0$$
$$\lim_{\theta\to 0} \theta u_{v_b^*}(\theta) = \lim_{\theta\to 0} \sqrt{\theta} \ = 0,$$

which implies that $\theta v_b^*(\theta) = 0$ for $\theta \to 0$. It is straightforward to verify that $\frac{1}{2} < \theta \left(v_b^*\right)^2 < 1$ when $\theta \to 0$. We now consider the limit of $2\theta + u_{r_b}(\theta)$:

$$\begin{aligned}\lim_{\theta\to 0} \left(2\theta + u_{r_b}(\theta, v_b^*)\right) &= \lim_{\theta\to 0} 2(\theta v_b^*)(n_x - 1)\left(1 + 2\sqrt{d}(\theta v_b^*)\right) e^{-\theta(v_b^*)^2} \\ &= 0,\end{aligned}$$

which is the desired result and this completes the proof of Lemma 7.

13 Proofs for Section 8

13.1 Proof of Proposition 11

From Corollary 1 and Lemma 10 it follows that with $v_{\min} = 2\sqrt{d}$ we only have $u_{\lambda_{\max}}(\theta) > n_x$ when $2\theta + u_{r_b}(\theta) > n_x$ and $\theta > \frac{1}{2}$. The next lemma considers the case when $2\theta + u_{r_b}(\theta; n_x) = n_x$.

Lemma 17 *For $\theta > \frac{1}{2}$, $d \in \mathbb{Z}^+$, and $v_{min} = 2\sqrt{d}$, we have $2\theta + u_{r_b}(\theta; n_x) = n_x$ when $n_x = \hat{n}_x > 0$, where*

$$\hat{n}_x = \frac{2\theta - g_b(\theta)}{1 - g_b(\theta)}, \tag{86}$$

and $g_b(\theta)$ comes from Eq. (59).

Proof For $v_{\min} = 2\sqrt{d}$ we have from Eq. (57) $\theta_b^* = \frac{1+\sqrt{5}}{8d} < \frac{1}{2}$ since $d \in \mathbb{Z}^+$. As such, from Lemma 5, $v_b(\theta) = v_{\min} = 2\sqrt{d}$ for $\theta \geq \frac{1}{2}$ and thus Eq. (59) is used:

$$\begin{aligned}2\theta + u_{r_b}(\theta; \hat{n}_x) &= 2\theta + (\hat{n}_x - 1)g_b \\ &= \hat{n}_x,\end{aligned}$$

where Eq. (86) is recovered by isolating for $\hat{n}_x$. Both the numerator and denominator of Eq. (86) are positive for $\theta > \frac{1}{2}$ thanks to Lemma 9 and this completes the proof.

We now evaluate $1 - u_{r_a}(\theta; \hat{n}_x)$ using Eqs. (58) and (86):

$$\begin{aligned}1 - u_{r_a}(\theta; \hat{n}_x) &= 1 - (\hat{n}_x - 1)g_a \\ &= \frac{1 - \left(2\theta(2\sqrt{d} + 1) - 1\right)(4d\theta + 1)e^{-4d\theta}}{1 - g_b} \\ &= \frac{1 - h_a(\theta; d)}{1 - g_b},\end{aligned} \tag{87}$$

where the denominator is always positive thanks to Lemma 9 and $h_a(\theta;d) = \left(2\theta(2\sqrt{d}+1)-1\right)(4d\theta+1)\,e^{-4d\theta}$. The maximum of $h_a(\theta;d)$ is considered in the following lemma.

Lemma 18 *For $\theta > \frac{1}{2}$ and $d \in \mathbb{Z}^+$ we have $h_a(\theta,d) \leq u_{h_a}(\theta;d) < 1$, where*

$$u_{h_a}(d) = (8\theta d - 2)(4\theta d + 1)e^{-4\theta d}. \tag{88}$$

Proof We start by showing that $u_{h_a}(d) \geq h_a(\theta;d)$:

$$\begin{aligned}(8\theta d - 2)(4\theta d + 1)e^{-4\theta d} &\geq \left(2\theta(2\sqrt{d}+1)-1\right)(4d\theta+1)\,e^{-4d\theta}\\ 2\theta(4d - 2\sqrt{d} - 1) &\geq 1.\end{aligned} \tag{89}$$

For $\theta > \frac{1}{2}$ and $d \in \mathbb{Z}^+$ the LHS is minimized and equal to one with $\theta = \frac{1}{2}$ and $d = 1$. We now calculate the maximum of $u_{h_a}(\theta,d)$ using $a = 4\theta d$, where $a \geq 2$ since $\theta > \frac{1}{2}$ and $d \in \mathbb{Z}^+$. The maximum of $u_{h_a}(a)$ is at

$$\begin{aligned}\frac{\partial u_{h_a}}{\partial a} &= \frac{\partial\left((a^2-1)e^{-a}\right)}{\partial a}\\ &= -2\left(a^2 - 2a - 1\right)e^{-1} = 0\\ a &= 1+\sqrt{2},\end{aligned} \tag{90}$$

where we only keep the positive root of the quadratic and it straightforward to verify that this is the location of a maximum. The maximum of $u_{h_a}(a)$ is thus $u_{h_a}(a = 1+\sqrt{2}) \approx 0.432$, which completes the proof.

Since $h_a(\theta,d) < 1$ for $\theta > \frac{1}{2}$ and $d \in \mathbb{Z}^+$ it follows from Eq. (87) that $1 - u_{r_a}(\theta) > 0$ when $u_{\lambda_{\max}}(\theta) \geq n_x$, which completes the proof of Proposition 11.

13.2 Proof of Proposition 12

We follow the same approach used for the proof of Proposition 11 in Section 13.1 and begin by evaluating $2\theta - u_{r_b}(\theta;\hat{n}_x)$ using Eqs. (59) and (86):

$$\begin{aligned}2\theta - u_{r_b}(\theta;\hat{n}_x) &= 2\theta - (\hat{n}_x - 1)g_b\\ &= \frac{2\theta}{1-g_b}\left[1 - 2\sqrt{d}(4\theta-1)\,(4\theta d+1)\,e^{-4d\theta}\right]\\ &= \frac{2\theta}{1-g_b}\left(1 - h_b(\theta,d)\right),\end{aligned} \tag{91}$$

where $h_b(\theta,d) = 2\sqrt{d}(4\theta-1)\,(4\theta d+1)\,e^{-4d\theta}$ and the denominator is positive as a result of Lemma 9. In order to have $2\theta - u_{r_b}(\theta;\hat{n}_x) > 0$ for $\theta > \frac{1}{2}$ we need to prove that $h_b(\theta,d) < 1$ for $d \in \mathbb{Z}^+$ and $\theta > \frac{1}{2}$. We begin by showing that $h_b < u_{h_a}$ for $d \in \mathbb{Z}^+$ and $\theta > \frac{1}{2}$, where u_{h_a} comes from Eq. (88):

$$\begin{aligned}(8\theta d - 2)(4\theta d + 1)e^{-4\theta d} &\geq 2\sqrt{d}\,(4\theta-1)\,(4d\theta+1)\,e^{-4d\theta}\\ (8\theta\sqrt{d} + 2)(\sqrt{d} - 1) &> 0,\end{aligned}$$

which is satisfied for $\theta > 0$ and $d \in \mathbb{Z}^+$. From Lemma 18 we have $u_{h_a}(\theta, d) \leq 1$ for $d \in \mathbb{Z}^+$ and $\theta > \frac{1}{2}$. Therefore, $h_b < u_{h_a} < 1$ for $d \in \mathbb{Z}^+$ and $\theta > \frac{1}{2}$. Since $h_b < 1$, it follows from Eq. (91) that $2\theta - u_{r_b}(\theta; n_x) > 0$ when $u_{\lambda_{\max}}(\theta) \geq n_x$, which completes the proof of Proposition 12.

14 Proofs for Section 9

14.1 Proof of Proposition 13

Eq. (63) is derived by setting $\theta = \frac{1}{2}$ in $2\theta - u_{r_b}(\theta, v_b(\theta)) = 0$ along with the constraint $v_{\min} \geq \sqrt{2}$. The solution to Eq. (63) thus satisfies all the criteria from Lemma 11 to ensure $\ell_{\lambda_{\min}} > 0 \,\forall\, \theta > \frac{1}{2}$, $(d, n_x) \in (\mathbb{Z}^+, \mathbb{Z}^+ \setminus 1)$. In order for the solution to Eqs. (61) and (63) to be the same, we must show that the solution to Eq. (63) is the smallest one that ensures $\ell_{\lambda_{\min}}(\theta; d, n_x) > 0 \,\forall\, \theta > \frac{1}{2}$, $(d, n_x) \in (\mathbb{Z}^+, \mathbb{Z}^+ \setminus 1)$.

Eq. (63) is simply $u_{r_b}(\theta, v) = 1$ with $v = v_{\text{req}} > \sqrt{2}$ and $\theta = \frac{1}{2}$. The function $u_{r_b}(\theta, v)$ evaluates to zero for $v = 0$ and $v \to \infty$ and from Proposition 9 we know it is a quasiconcave function with respect to v. Therefore, if there is a value of $v > 0$ such that $u_{r_b}(\theta, v) > 1$, then there are two values of v that satisfy $u_{r_b}(\theta, v) = 1$, one smaller and one greater than $\sqrt{2}$ and v_b^*. With $d = 1$, $n_x = 2$, and $v = \sqrt{2}$ we have $u_{r_b} \approx 1.26$. Since u_{r_b} is monotonically increasing with respect to both d and n_x, it follows that there are two values of v that satisfy $u_{r_b}(\theta, v) = 1$ for $d \in \mathbb{Z}^+$ and $n_x \in \mathbb{Z}^+ \setminus 1$. However, only the larger solution is greater than v_b^* and ensures $u_{r_b}(\theta, v_b) = 1$ since for the smaller solution we have $v_b = v_b^*$ and thus $u_{r_b}(\theta, v_b) > 1$. Therefore, the requirement in Eq. (63) that $v_{\min} \geq v_{\text{req}} > \sqrt{2}$ ensures that the larger solution of $u_{r_b}(\theta, v) = 1$ is found. With $v_{\min} = v_{\text{req}}$ we thus have the smallest value of $v_{\min}$ that ensures $u_{r_b}(\theta, v_b) = 1$ and thus $\ell_{\lambda_{\min}}(\theta) = 0$ at $\theta = \frac{1}{2}$. The next two lemmas prove that with $v_{\min} \geq v_{\text{req}}$, the bound $\ell_{\lambda_{\min}}(\theta)$ is monotonically increasing for $\theta > \frac{1}{2}$.

Lemma 19 *The solution to Eq. (63) ensures that $\ell_{\lambda_{min}}(\theta)$ is monotonically increasing for $\theta \geq \frac{1}{2}$ and $(d, n_x) \in (\mathbb{Z}^+, \mathbb{Z}^+ \setminus 1) \setminus (1, 2)$.*

Proof The solution to Eq. (63) for $(d, n_x) = (1, 3)$ and $(d, n_x) = (2, 2)$ is $v_{\text{req}} = 2.347$ and $v_{\text{req}} = 2.031$, respectively. The LHS of Eq. (63) is monotonically increasing with respect to d and n_x but monotonically decreasing with respect to v_{req} since $v_{\text{req}} > v_b^*$. Therefore, since the RHS of Eq. (63) is constant, v_{req} must be monotonically increasing with respect to d and n_x. As such $v_{\text{req}} > 2$ for $(d, n_x) \in (\mathbb{Z}^+, \mathbb{Z}^+ \setminus 1) \setminus (1, 2)$ and Lemma 12 indicates this is a sufficient condition to have $\ell_{\lambda_{\min}}(\theta)$ be monotonically increasing for $\theta \geq \frac{1}{2}$, which completes the proof.

Lemma 20 *The solution to Eq. (63) ensures that $\ell_{\lambda_{min}}(\theta)$ is monotonically increasing for $\theta \geq \frac{1}{2}$ and $(d, n_x) = (1, 2)$.*

Proof A sufficient condition for $\ell_{\lambda_{\min}}(\theta)$ to be monotonically increasing for $\theta > \frac{1}{2}$ is that both $1 - u_{r_a}(\theta)$ and $2\theta - u_{r_b}(\theta)$ are themselves monotonically increasing for $\theta > \frac{1}{2}$. The solution to Eq. (63) with $(d, n_x) = (1, 2)$ is $v_{\text{req}} = 1.797$. From Eq. (37) we have $\theta_a^*(v = 1.797, d = 1) = 0.031$, which indicates $1 - u_{r_a}(\theta)$ is monotonically increasing for $\theta > \frac{1}{2}$. We now differentiate $2\theta - u_{r_b}(\theta; d = 1, n_x = 2)$:

$$\frac{\partial \left(2\theta - u_{r_b}(\theta)\right)}{\partial \theta} = 2 + 2v_{\min}\left(2v_{\min}^3\theta^2 + v_{\min}(v_{\min} - 4)\theta - 1\right)e^{-\theta v_{\min}^2}. \quad (92)$$

For $v_{\min} = v_{\text{req}} = 1.797$ we have $\frac{\partial\left(2\theta - u_{r_b}(\theta)\right)}{\partial\theta} = 0$ only when $\theta = 0.224$. Therefore, $2\theta - u_{r_b}(\theta; d = 1, n_x = 2)$ is monotonically increasing for $\theta > 0.224$, which completes the proof.

The solution to Eq. (63) is the smallest one that ensures $\ell_{\lambda_{\min}}(\theta) = 0$ for $\theta = \frac{1}{2}$ and it is also sufficiently large to ensure $\ell_{\lambda_{\min}}(\theta)$ is monotonically increasing for $\theta > \frac{1}{2}$. Therefore, the solution to Eq. (63) is the solution to Eq. (61), which completes the proof.

14.2 Proof of Proposition 14

We take the natural logarithm of both sides of Eq. (63):

$$\ln\left((n_x - 1)v\left(1 + \sqrt{d}v\right)e^{-\frac{v^2}{2}}\right) = \ln(1),$$

and isolate v^2 to obtain

$$v^2 = 2\ln(n_x - 1) + 2\ln(v) + 2\ln(1 + \sqrt{d}v). \quad (93)$$

The two following lemmas provide upper bounds on the two non-polynomial terms in Eq. (93) that contain v.

Lemma 21 *For $v \geq 2$ and $d \in \mathbb{Z}^+$ we have*

$$\ln(v) + \ln\left(\frac{1 + 2\sqrt{d}}{2}\right) \geq \ln\left(1 + \sqrt{d}v\right). \quad (94)$$

Proof We start by finding the smallest value of c_1 such that the following inequality holds for $v > 2$ and $d \in \mathbb{Z}^+$:

$$\ln(c_1\sqrt{d}v) \geq \ln(1 + \sqrt{d}v) \quad (95)$$

$$c_1 = \max_{v \geq 2} \frac{1 + \sqrt{d}v}{\sqrt{d}v}$$

$$= \frac{1 + 2\sqrt{d}}{2\sqrt{d}}, \quad (96)$$

where the minimum value of v, i.e. $v = 2$, was used since $\frac{1+\sqrt{d}v}{\sqrt{d}v} = \frac{1}{\sqrt{d}v} + 1$ is monotonically decreasing with respect to v. Eq. (94) is recovered by substituting the value of c_1 from Eq. (96) into Eq. (95), which completes the proof.

Lemma 22 *For $v > 0$ we have $\frac{v}{e} \geq \ln(v)$.*

Proof We have $\max \frac{\ln(v)}{v} = \frac{1}{e}$ at $v = e$. Therefore, $\frac{v}{e} \geq \ln(v) \, \forall \, v > 0$, which completes the proof.

We now use Lemmas 21 and 22 to convert Eq. (93) into an algebraic equation:

$$\begin{aligned} v^2 &> 2\ln(v) + 2\ln(n_x - 1) + 2\left[\ln(v) + \ln\left(\frac{1+2\sqrt{d}}{2}\right)\right] \\ &> \frac{4}{e}v + 2\ln\left(\frac{(n_x-1)\left(1+2\sqrt{d}\right)}{2}\right), \end{aligned} \tag{97}$$

which is a quadratic relation that can be satisfied with the positive root of the quadratic equation:

$$\tilde{v}_{\text{req}}(d, n_x) = \frac{2 + \sqrt{4 + 2e^2 \ln\left(\frac{(n_x-1)\left(1+2\sqrt{d}\right)}{2}\right)}}{e}, \tag{98}$$

which matches Eq. (64). Lemma 21 considered the case with $v \geq 2$ but $\tilde{v}_{\text{req}}(n_x = 2, d = 1) = 1.899$. Nonetheless, $v_{\text{req}}(n_x = 2, d = 1) = 1.814$ and as such, $\tilde{v}_{\text{req}} \geq v_{\text{req}} \, \forall (d, n_x) \in (\mathbb{Z}^+, \mathbb{Z}^+ \setminus 1)$. From Proposition 13 it follows that $v_{\min} \geq v_{\text{req}}$ ensures that $\ell_{\lambda_{\min}}$ is positive and monotonically increasing for $\theta > \frac{1}{2}$, which satisfies the constraint in Eq. (61) and this completes the proof of Proposition 14.

14.3 Proof of Proposition 15

We consider the maximum of $u_{\lambda_{\max}}(\theta)$ for $0 < \theta \leq \frac{1}{2}$ using Eq. (36):

$$\begin{aligned} \max_{0<\theta\leq\frac{1}{2}} u_{\lambda_{\max}} &= \max_{0<\theta\leq\frac{1}{2}} \left(1 + u^*_{r_a}, 2\theta + u^*_{r_b}\right) \\ &\leq \max_{0<\theta\leq\frac{1}{2}} \left(1 + u^*_{r_a}, 1 + u^*_{r_b}\right). \end{aligned} \tag{99}$$

To prove that $u_{\lambda_{\max}} = 1 + u^*_{r_a}$ for $d \in \mathbb{Z}^+$, $n_x \in \mathbb{Z}^+ \setminus 1$, $0 < \theta \leq \frac{1}{2}$, and $v_{\text{req}} \leq v_{\min} \leq 2\sqrt{d}$ it is thus sufficient to show that the following relation is satisfied:

$$\begin{aligned} & u^*_{r_b}(v_{\min}) < u^*_{r_a}(v_{\min}) \\ 2(n_x - 1)\frac{4\sqrt{d} + \sqrt{v^2_{\min} + 16d}}{v^2_{\min}} e^{-\frac{4\sqrt{d} + \sqrt{v^2_{\min}+16d} - v_{\min}}{4\sqrt{d}}} &< (n_x - 1)\frac{2\sqrt{d}}{v_{\min}} e^{1 - \frac{v_{\min}}{2\sqrt{d}}} \\ \frac{\sqrt{d} v_{\min}}{4\sqrt{d} + \sqrt{v^2_{\min} + 16d}} e^{\left(\frac{v_{\min} + \sqrt{v^2_{\min}+16d}}{4\sqrt{d}}\right)} &> 1, \end{aligned} \tag{100}$$

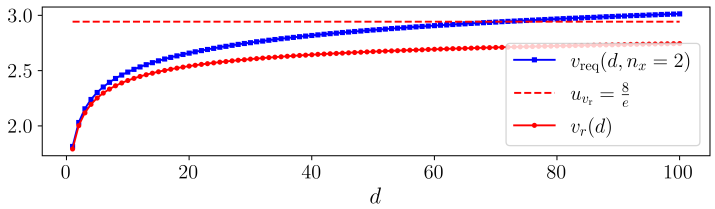

Fig. 14: Comparing v_{req} and v_r, which are the roots to Eqs. (63) and (100), respectively.

where Eqs. (42) and (51) were used for $u^*_{r_a}$ and $u^*_{r_b}$, respectively. To determine when Eq. (100) is satisfied the trend of the LHS of Eq. (100) with respect to v_{min} and d is required and this is considered in the two following lemmas.

Lemma 23 *The LHS of Eq. (100), which is denoted as $g(v_{min}, d)$, is monotonically increasing with respect to v_{min} for $v_{min} > 0$ and $d \in \mathbb{Z}^+$.*

Proof The derivative of $g(v_{\text{min}}, d)$ with respect to v_{min} is

$$\frac{\partial g}{\partial v_{\text{min}}} = \frac{\left(v_{\text{min}} + 4\sqrt{d}\right)\sqrt{v_{\text{min}}^2 + 16d} + 4\sqrt{d}v_{\text{min}} + 16d + v_{\text{min}}^2}{4\left(\sqrt{v_{\text{min}}^2 + 16d} + 4\sqrt{d}\right)^2} e^{\left(\frac{v_{\text{min}} + \sqrt{v_{\text{min}}^2 + 16d}}{4\sqrt{d}}\right)}, \tag{101}$$

which is always positive for $v_{\text{r}} > 0$ and $d \in \mathbb{Z}^+$ and this completes the proof.

Lemma 24 *The LHS of Eq. (100), which is denoted as $g(v_{min}, d)$, is monotonically decreasing with respect to d for $v_r > 0$ and $d \in \mathbb{Z}^+$.*

Proof The partial derivative of $g(v_{\text{r}}, d)$ with respect to d is

$$\frac{\partial g}{\partial d} = -\frac{v_{\text{r}}\left(v_{\text{r}} + \sqrt{v_{\text{r}}^2 + 16d} - 4\sqrt{d}\right)}{8d\left(\sqrt{v_{\text{r}}^2 + 16d} + 4\sqrt{d}\right)} e^{\left(\frac{v_{\text{min}} + \sqrt{v_{\text{min}}^2 + 16d}}{4\sqrt{d}}\right)}, \tag{102}$$

which is always negative since $\sqrt{v_{\text{r}}^2 + 16d} - 4\sqrt{d} > 0$ for $v_{\text{r}} > 0$ and $d \in \mathbb{Z}^+$.

We are interested in proving that $u^*_{r_a}(v_{\text{min}}) > u^*_{r_b}(v_{\text{min}})$ for $v_{\text{min}} \geq v_{\text{req}}$. In order to do that the following lemma solves for v_{r}, which is the solution to $u^*_{r_a}(v_{\text{r}}) = u^*_{r_b}(v_{\text{r}})$. It is then proven that $v_{\text{req}} > v_{\text{r}}$, which ensures $u^*_{r_a}(v_{\text{req}}) > u^*_{r_b}(v_{\text{req}})$.

Lemma 25 *There is a unique solution v_r to the equation $u^*_{r_a}(v_r) = u^*_{r_b}(v_r)$, where $0 < v_r \leq u_{v_r} = \frac{8}{e}$.*

Proof From Lemma 23 we know that the LHS of Eq. (100), which is denoted as $g(v_{\min}, d)$, increases monotonically with respect to $v_{\min}$. As such, there is a unique $v_{\mathrm{r}}(d)$ that satisfies $g(v_{\mathrm{r}}) = 1$, which is equivalent to $u^*_{r_a}(v_{\mathrm{r}}) = u^*_{r_b}(v_{\mathrm{r}})$. We have $g(0) = 0$ and we therefore require $v_{\mathrm{r}} > 0$ to have $g(v_{\mathrm{r}}) = 1$. From Lemma 24 we know that $g(d)$ is monotonically decreasing with respect to d. As such, when d increases, the LHS decreases, and thus v_{r} must increase to ensure $g(v_{\mathrm{r}}) = 1$. This can be seen in Fig. 14. Since $v_{\mathrm{r}}(d)$ increases with respect to d, we consider the following limit:

$$\begin{aligned}\lim_{d\to\infty} g(v_{\mathrm{r}}; d) &= \lim_{d\to\infty} \left(\frac{v_{\mathrm{r}}}{4 + \sqrt{\frac{v_{\mathrm{r}}^2}{d} + 16}} \right) e^{\left(\frac{\frac{v_{\mathrm{r}}}{\sqrt{d}} + \sqrt{\frac{v_{\mathrm{r}}^2}{\sqrt{d}} + 16}}{4} \right)} \\ &= \frac{v_{\mathrm{r}}}{8} e. \end{aligned} \tag{103}$$

For $d \in \mathbb{Z}^+$ it follows that there is a unique value of v_{r} such that $u^*_{r_a}(v_{\mathrm{r}}) = u^*_{r_b}(v_{\mathrm{r}})$, where $v_{\mathrm{r}} \in \left(0, \frac{8}{e}\right]$, which completes the proof.

As explained in the proof of Lemma 19, $v_{\mathrm{req}}(d, n_x)$ increases monotonically with respect to d and n_x and is thus minimized with $n_x = 2$. We thus want to show that $v_{\mathrm{req}}(d, n_x = 2) > v_{\mathrm{r}}(d) \, \forall d \in \mathbb{Z}^+$ and this will also hold for all $n_x \in \mathbb{Z}^+ \setminus 1$. Fig. 14 shows that for $1 \leq d \leq 100$ we have $v_{\mathrm{req}}(d, n_x = 2) > v_{\mathrm{r}}$. For $d = 100$ we have $v_{\mathrm{req}}(d, n_x = 2) > u_{v_{\mathrm{r}}}$ and this holds for all $d > 100$ since $v_{\mathrm{req}}(d)$ is monotonically increasing with respect to d. We thus have $v_{\mathrm{req}}(d, n_x) > v_{\mathrm{r}}(d) \, \forall \, (d, n_x) \in (\mathbb{Z}^+, \mathbb{Z}^+ \setminus 1)$ and it follows from Eq. (100) that $u^*_{r_a}(v_{\min}) > u^*_{r_b}(v_{\min})$ when $v_{\min} \geq v_{\mathrm{req}}$, which completes the proof of Proposition 15.